Physical Processes in the Radiation Belts: 10 Years of GEM IMS Accomplishments

Richard M. Thorne

Department of Atmospheric and Oceanic Sciences, UCLA

- Briefly review the structure of the radiation belts and the concept of adiabatic motion.
- Present evidence for non-adiabatic processes.
- Review our understanding or processes prior to 1996.
- Summarize GEM IMW WG2 accomplishments (1996-2006)
- Describe selected GEM campaign studies based on recent observational, theory and modeling studies of energetic electron variability.

Student Sponsored Tutorial, GEM, Snowmass, June 2006

Van Allen Radiation Belts

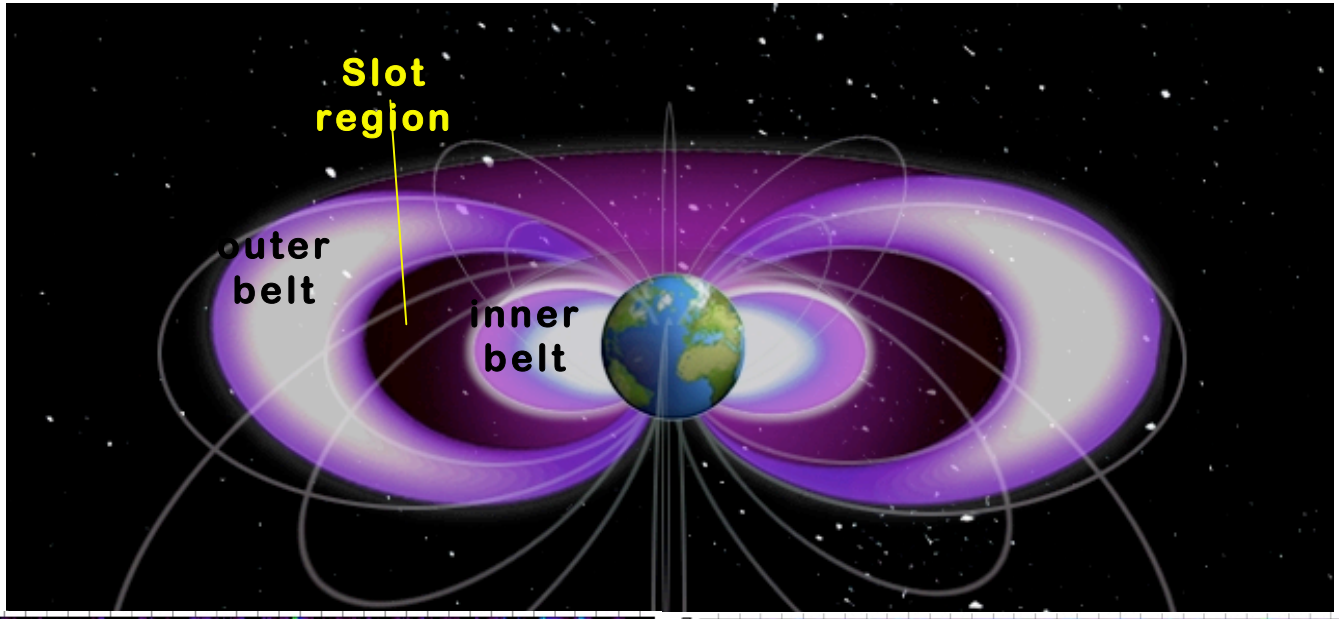

M. Hudson
J. Goldstein

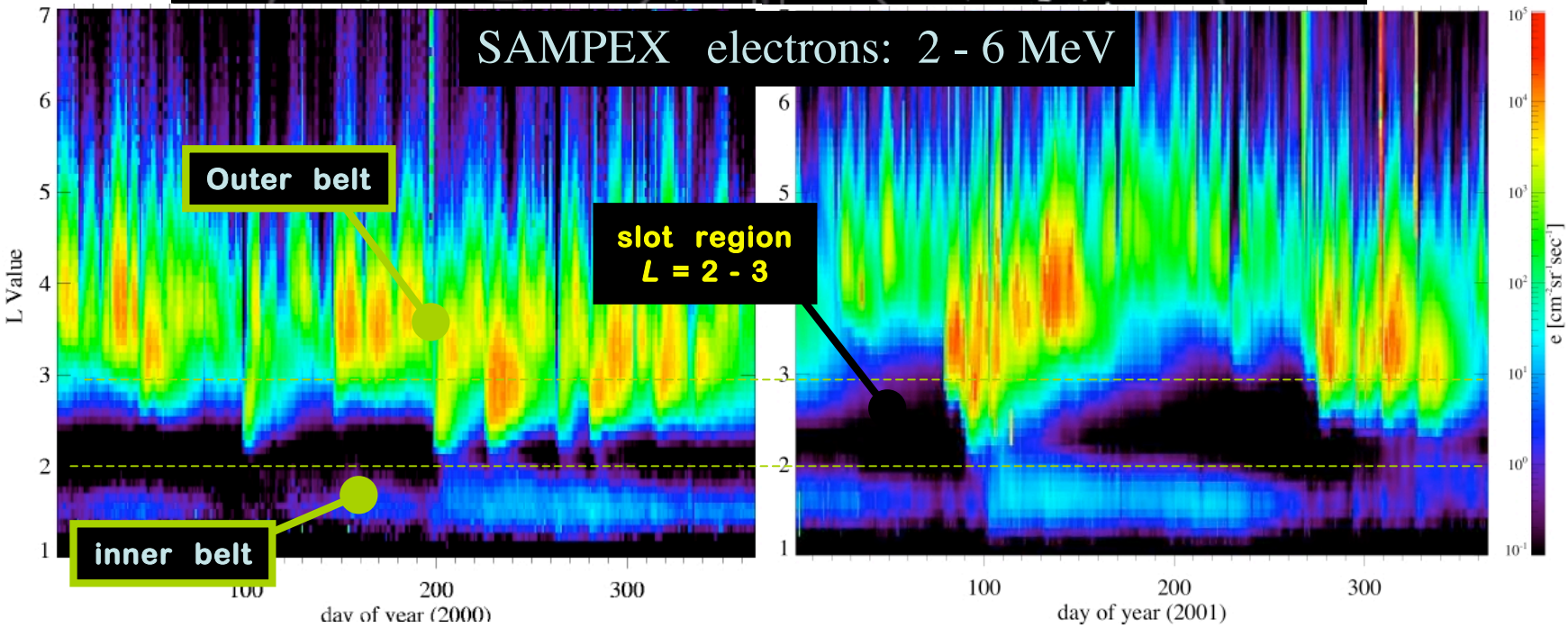

SAMPEX MeV Electron Variability and the Association with Solar Activity and the Plasmapause Location

Strongest Acceleration during fast SW streams

Li et al., GRL in press

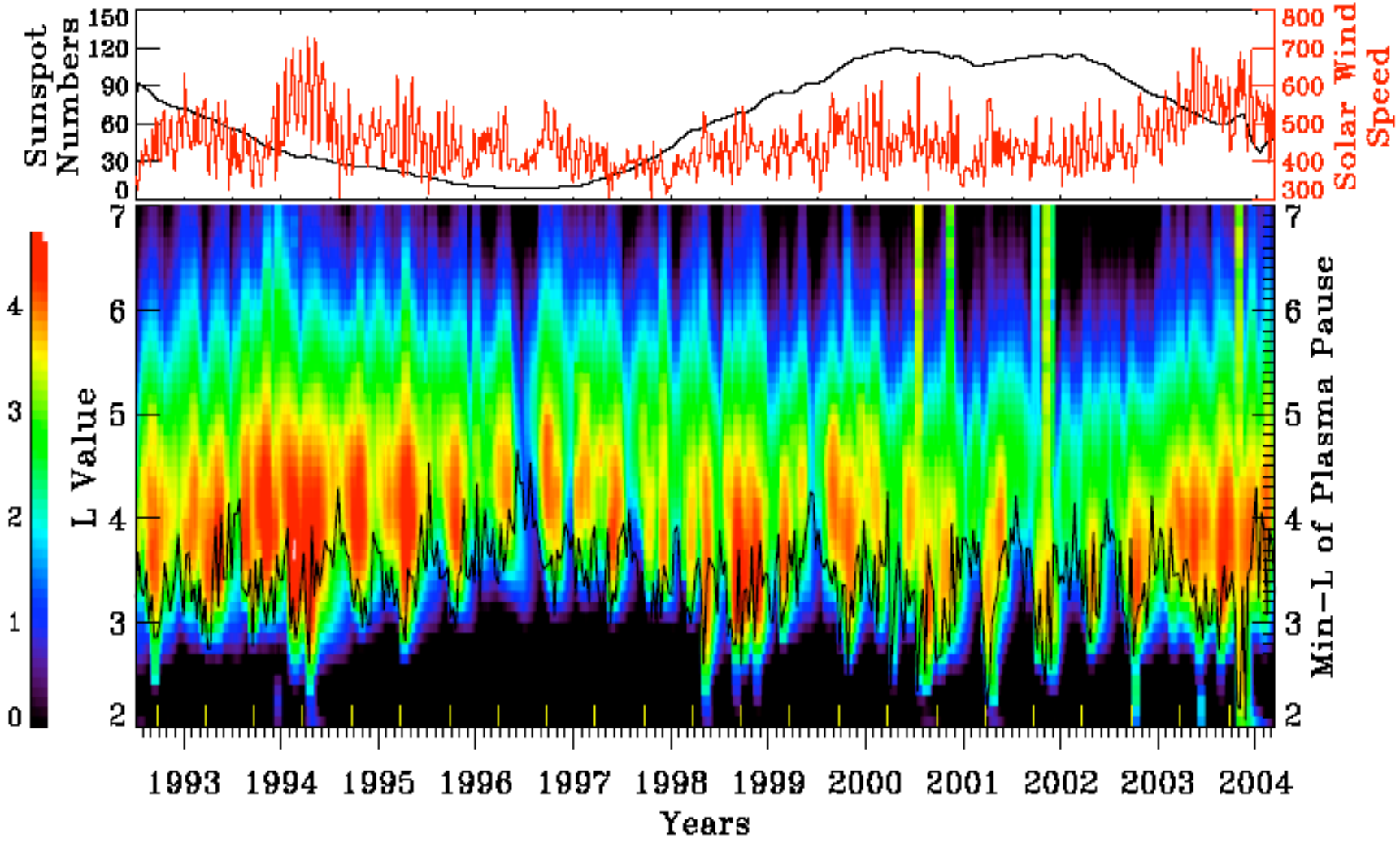

Electron Variability over the Solar Cycle

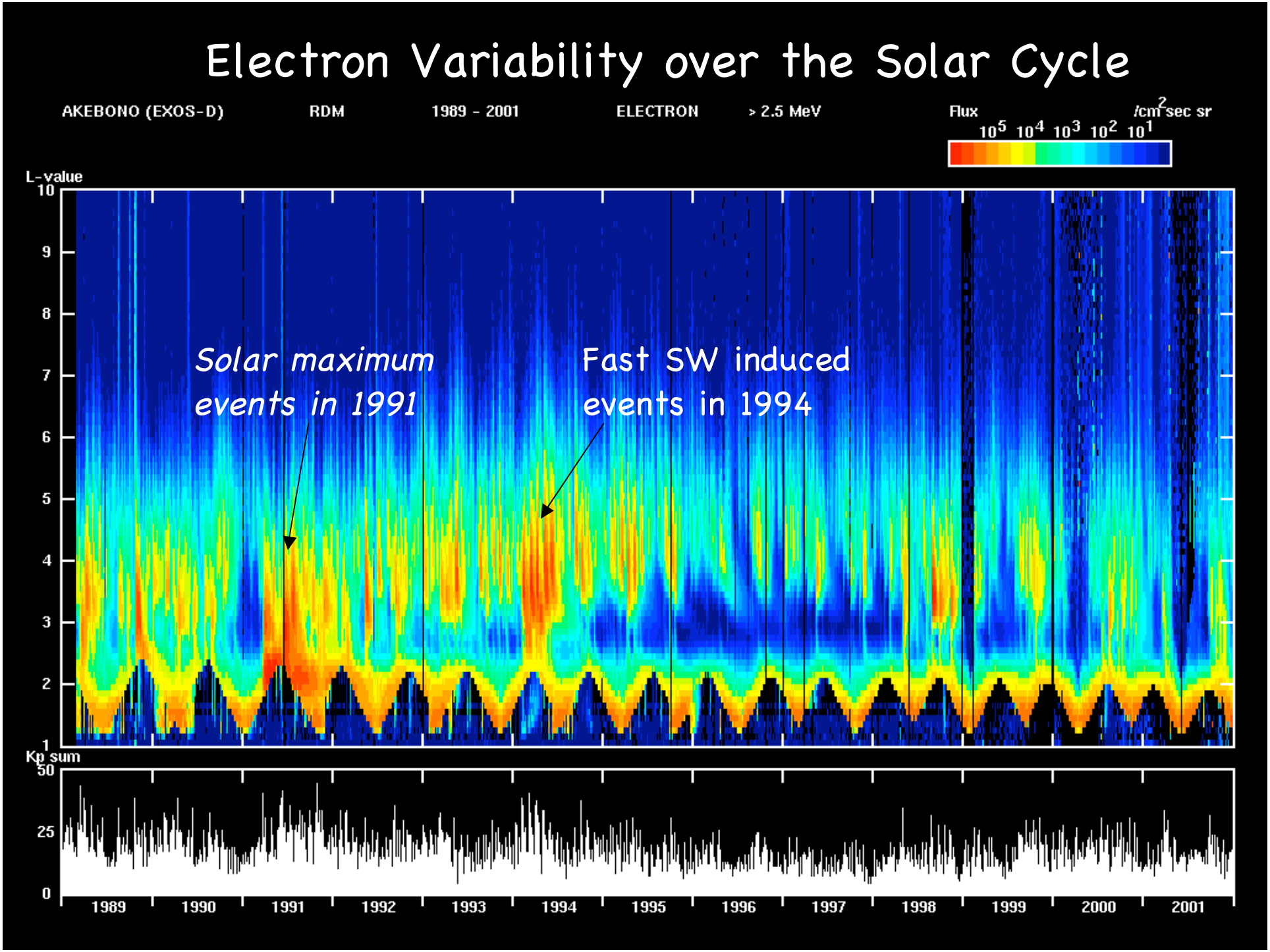

What are the Principal Drivers of Energetic Electron Variability?

Geomagnetic Activity Over the 27 day Solar Rotation Cycle in 2003 from Kyoto website

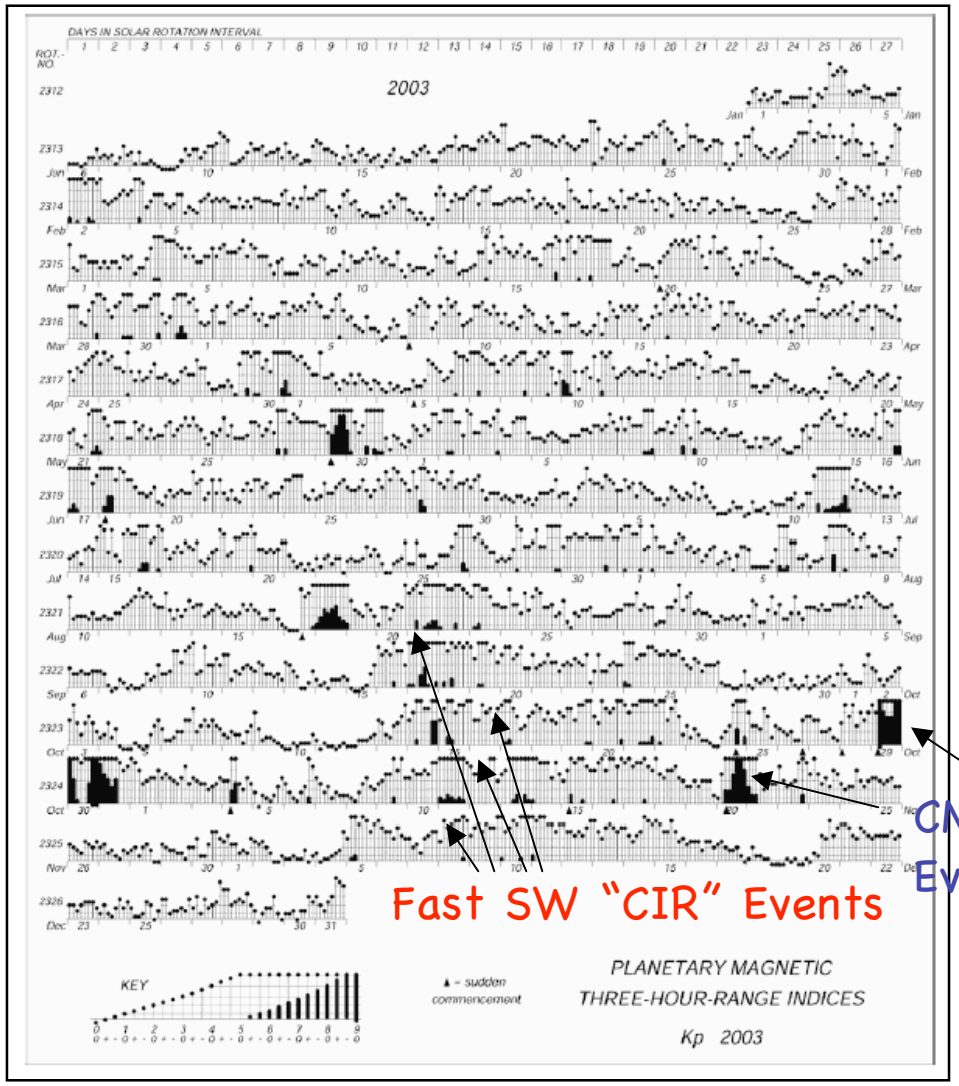

Fast SW "CIR" Events

CME Events

Akebono RDM > 2.5 MeV

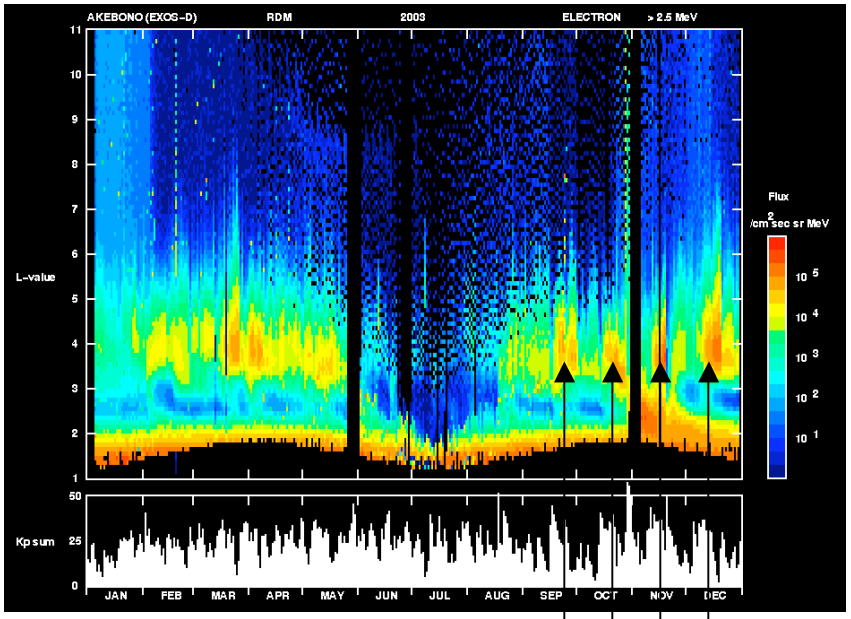

CIR Events

Extended periods of enhanced geomagnetic activity following CIR events leads to enhanced outer zone electron flux.

CME's can induce more intense electron acceleration at lower L but can also cause a net loss at L~4

Radiation Belts: Adiabatic Motion

Three adiabatic invariants of the particle motion are associated with the gyro, bounce, and drift motion of particles as illustrated below.

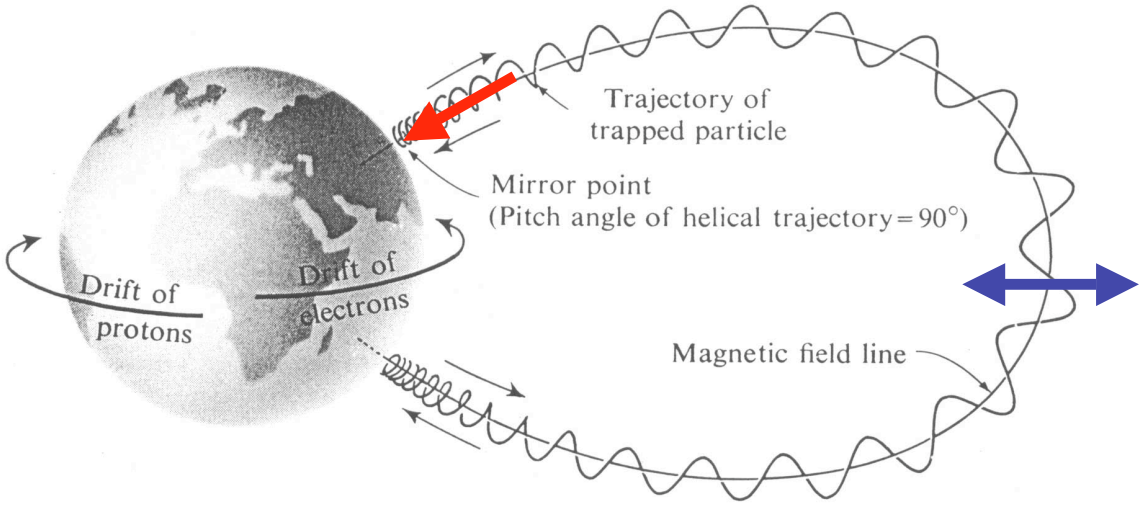

Violation of adiabatic motion by wave-particle interactions require waves with periods comparable to the periodic motion.

Invariants of the motion: time-scales for violation

$\mu = p_\perp^2 / 2mB$: $\tau_G \approx$ milli secs

$J = \oint_{bounce} p_\parallel dl$: $\tau_B \approx$ sec

$\Phi = \oint_{drift} B dA$: $\tau_D \sim 10$ min $(\gamma \gg 1)$

Scattering loss to atmosphere, and local acceleration

Radial diffusion by ULF waves

Some Magnetospheric Plasma Waves Responsible for Electron 1st Invariant Violation

Meredith et al, JGR 2004

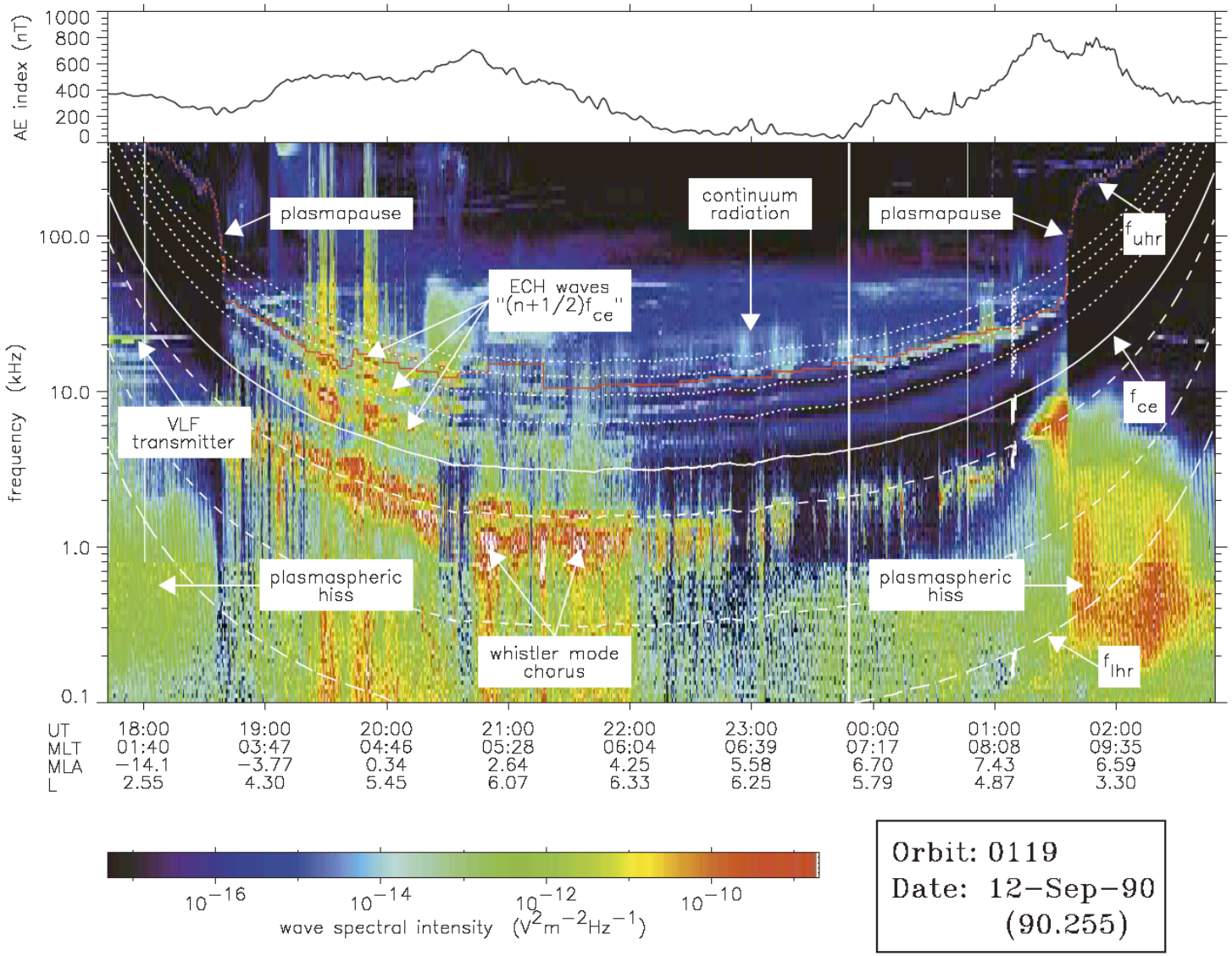

Whistler-mode Chorus and Hiss

Wave Excitation is controlled by the Plasmapause

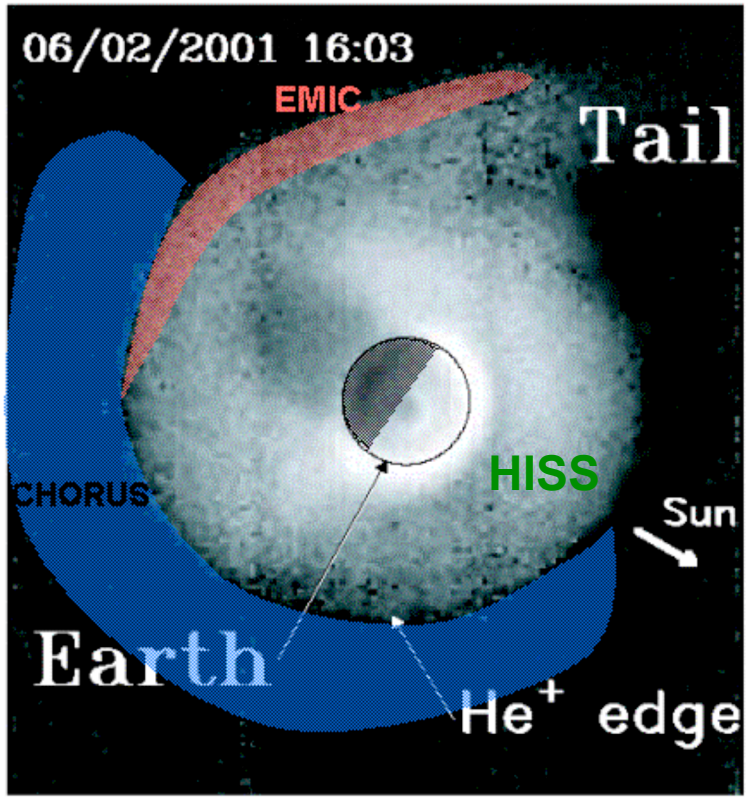

Paul O'Brien

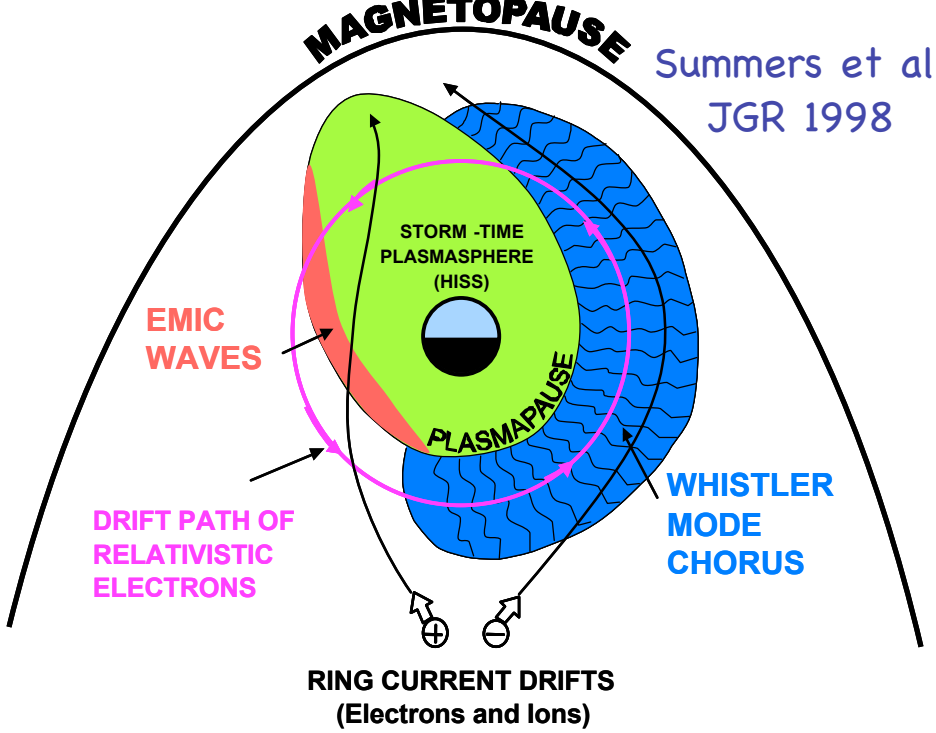

- Whistler-mode Hiss is found throughout the plasmasphere
- EMIC are found on the outer plasmasphere and in plumes, where injected hot ions encounter cold, dense plasma
- Whistler-mode Chorus is found outside the plasmapause, associated with freshly injected hot electrons

What was the State of Our Understanding of Radiation Belt Dynamics at the Start of the GEM IMS campaign in 1996?

1. Detailed observations of radiation belt structure.
2. Concept of stable trapping [Kennel and Petschek, 1966] to account for the observed limit on outer belt fluxes.
3. Quantitative analysis of electron loss rates inside the plasmapause [Lyons et al., 1972: Albert, 1994].
4. Empirical and data derived models for radial diffusion.
5. Basic mechanism for formation of the slot between the electron belts [Lyons and Thorne, 1973].
6. Affect of EMIC waves on RC ions and relativistic electrons [Cornwall et al, 1970; Thorne and Kennel, 1973].
7. Adiabatic variation during storms [Kim and Chan, 1997].
8. Rapid drift resonant acceleration associated with interplanetary shocks [Li et al., 1993].

GEM IMS WG2 (Radiation Belts) Accomplishments (1996-2006)

1. Comparative role of scattering by different waves inside the plasmasphere

2. Quantitative analysis of radial diffusion by ULF waves.

3. Quantification of outer zone electron precipitation loss by EMIC and chorus emissions during storm conditions.

4. Quantification of local acceleration by chorus emissions.

5. Global modeling of ring current ion and electron injection and associated wave excitation.

6. Analysis of radial profiles of phase space density.

7. Development of 2D and 3D kinetic diffusion codes.

Quiet-Time Structure of the Electron Belts

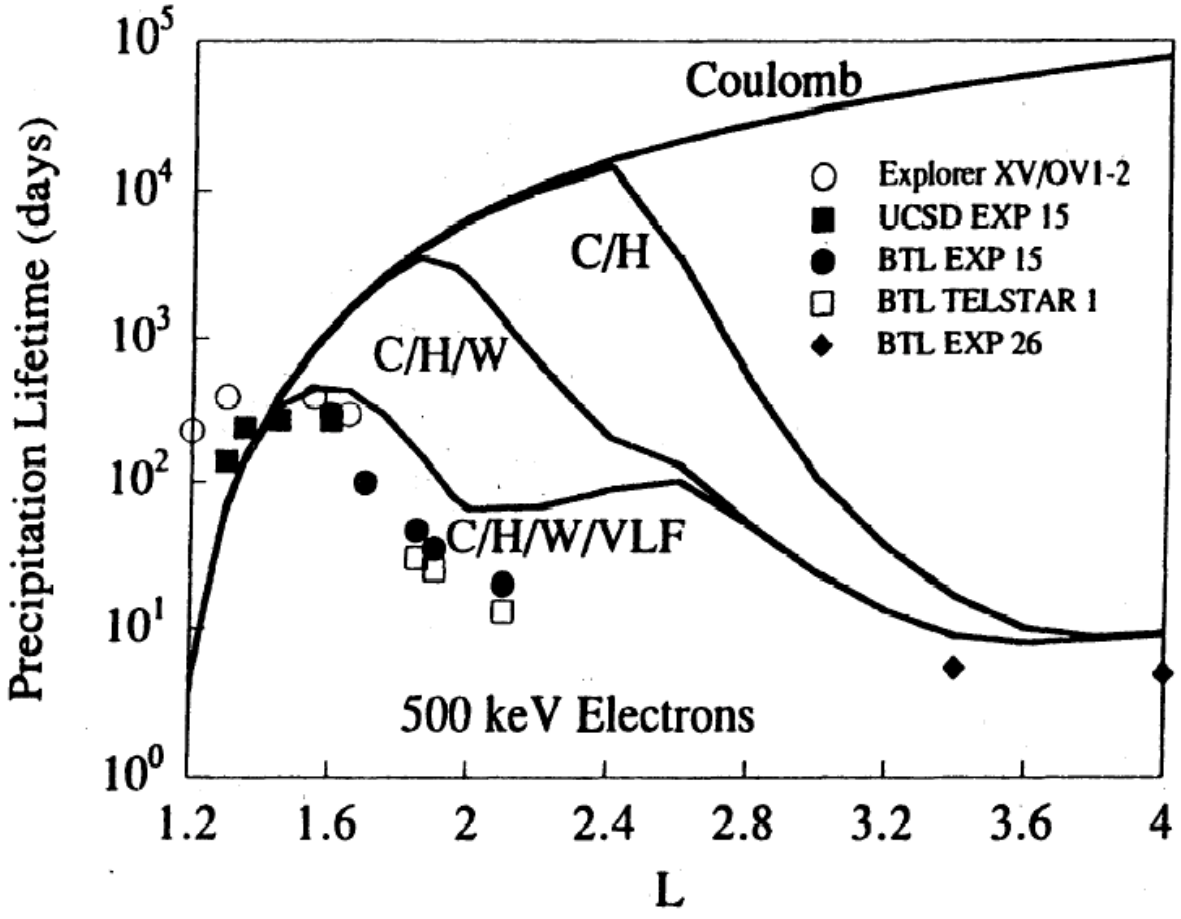

C - Coulomb Scattering
H – Hiss

W – Lightning Whistlers
VLF – VLF transmitters

Abel and Thorne, JGR, 103, 2385, 1998

- Loss of energetic electrons from the inner magnetosphere is determined by a combination of different processes:
  - Coulomb scattering,
  - Plasmaspheric hiss,
  - Lightning-generated whistlers,
  - and VLF transmitters

Natural Variations in the Outer Zone and the Physical Processes that Produce them

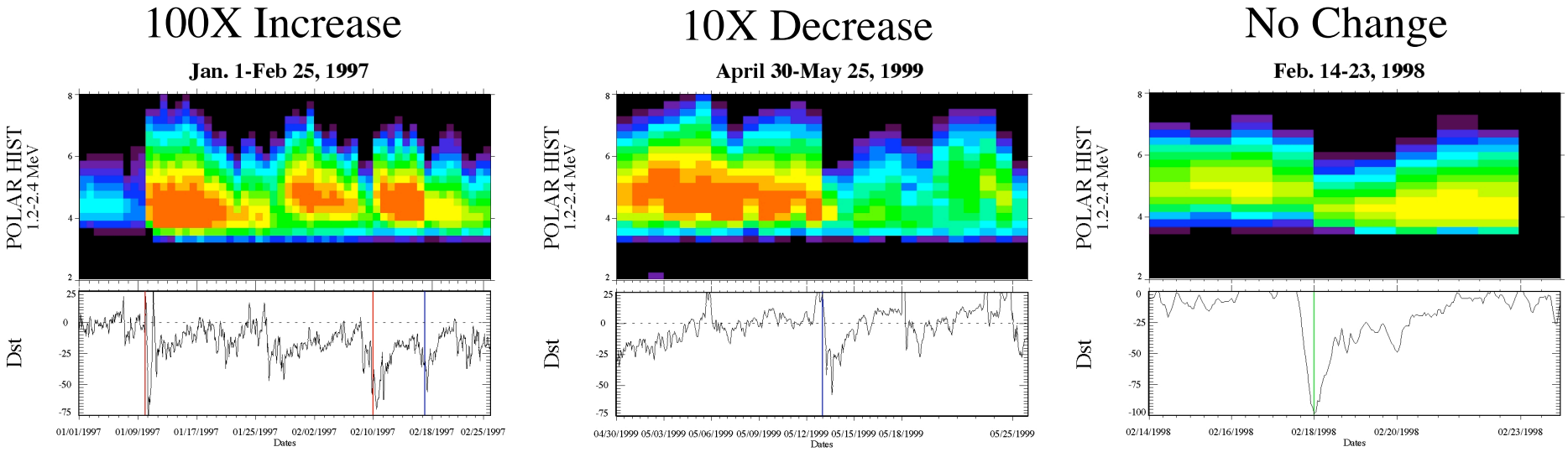

Reeves et al., JGR 2003

- How do electrons get accelerated to MeV energies in the outer radiation belt?
- What processes operate during storms to both create and destroy the radiation belts?

Electron Flux Change During Magnetic Storms

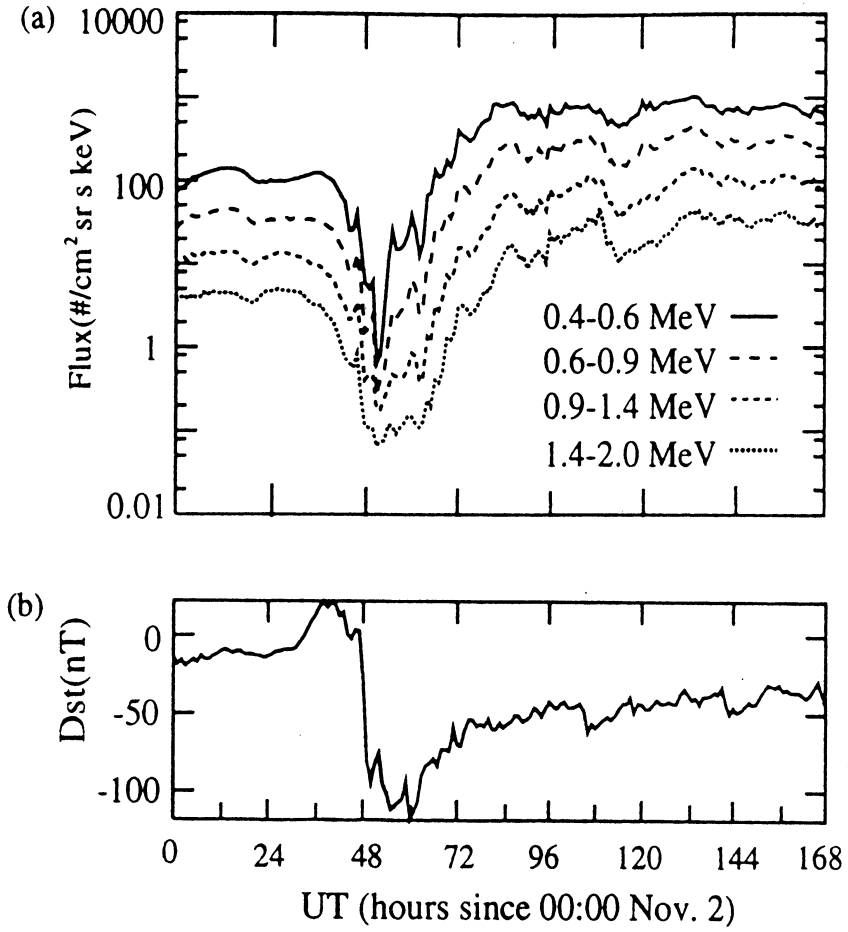

Figure 1. (a) Hourly averaged electron flux variation at GEO for November 2–8, 1993, measured by the CPA instrument on the LANL spacecraft 1984–129 (LT = UT + 0.5) for four high-energy channel and (b) *Dst* variation for the same time period.

- MeV flux drops rapidly during storm main phase (as measured by Dst)
- Flux increases during recovery phase
- Fluxes often increase above pre-storm level before Dst recovered
- Net acceleration on timescale ~ 1-2 days

Anticipated Changes in Phase Space Density during Acceleration, Transport & Loss

Geoff Reeves

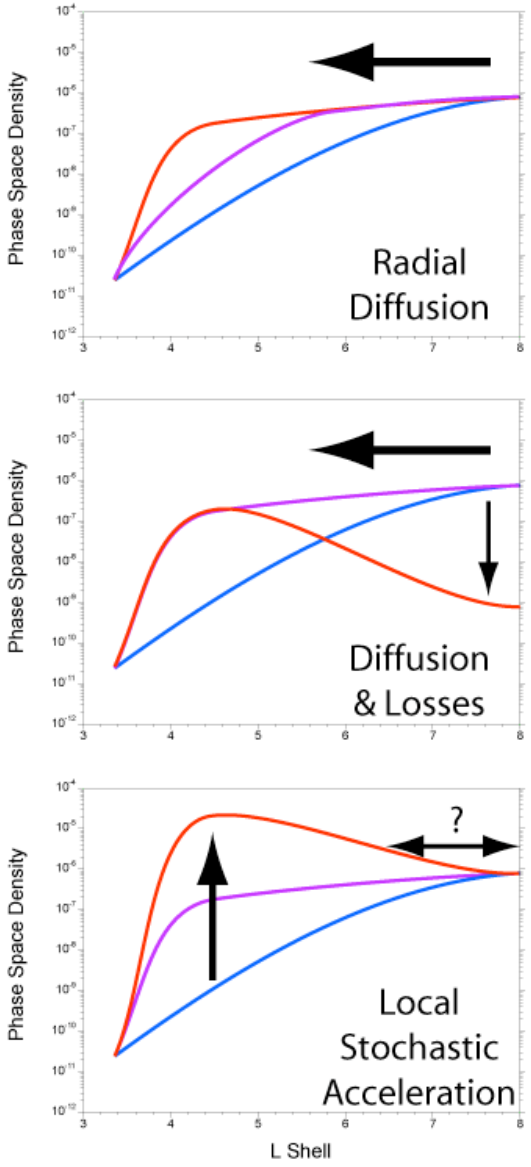

Enhanced radial diffusion by stormtime ULF waves leads to inward transport and acceleration and a monotonic gradient in PSD

Depletion in the outer magnetosphere following inward diffusion can lead to a PSD peak

Local acceleration produces peaks in PSD, which are subsequently smoothed by radial diffusion

1. Resonant Interactions with Plasmaspheric Hiss

$$\omega - k_{ll} v_{ll} = n \Omega_{gyro}/\gamma$$

Landau resonance; n=0
Cyclotron resonance; n=1, 2, 3 etc

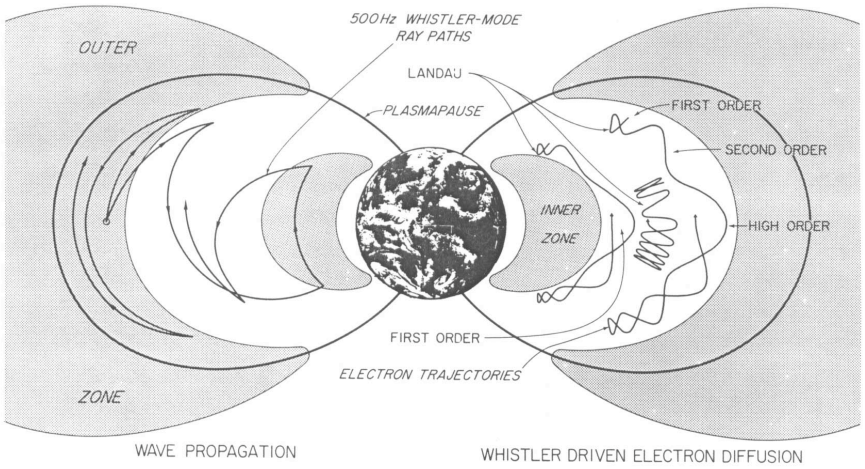

Lyons et al., 1972

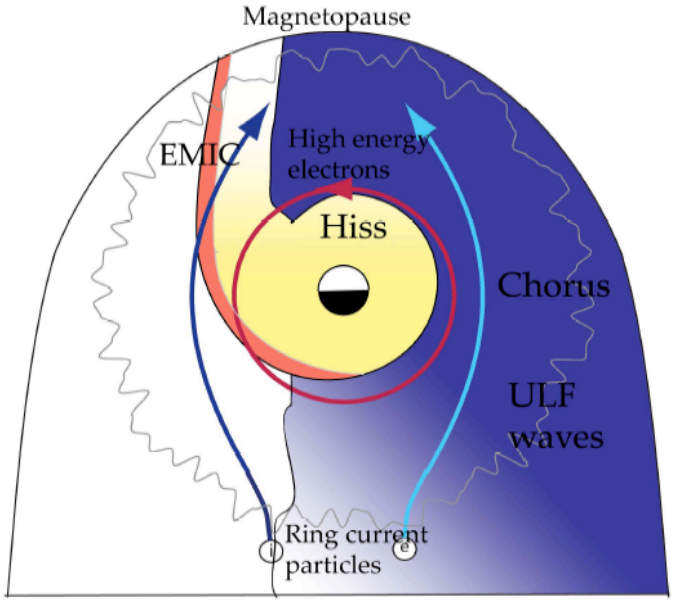

Schematic by Yuri Shprits

Resonant wave-particle interactions with plasmaspheric hiss primarily cause pitch-angle scattering (loss to the atmosphere)

Hiss Properties:

B_{wave} ~ 30 pT

$\omega/\Omega_e < 0.1$

Weak diffusion

Electron Decay Rates in the Inner Magnetosphere Following Stormtime Injection: Meredith et al., JGR 2005

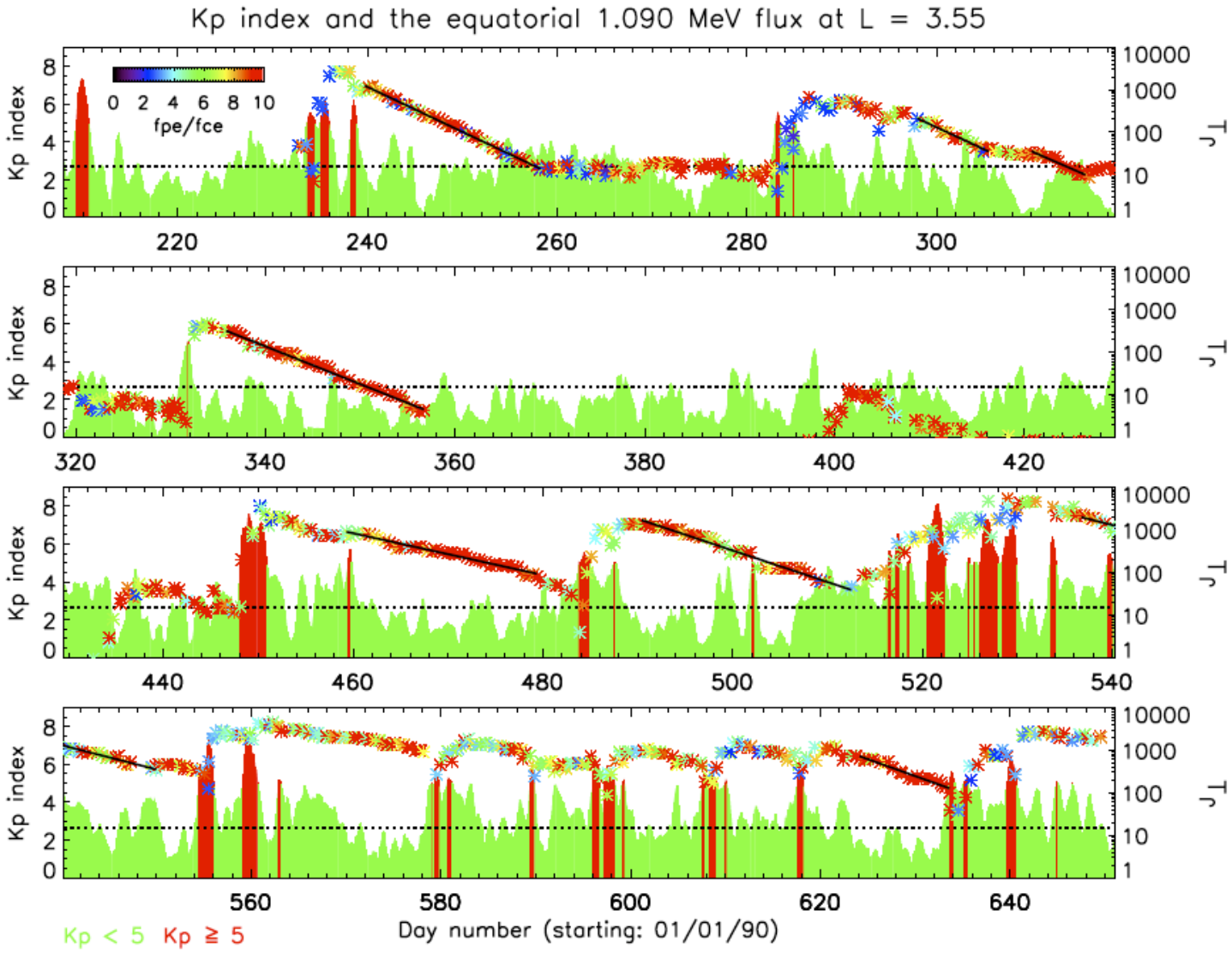

Quiet Time Loss Times Inside the Plasmasphere

Meredith et al., JGR 2005

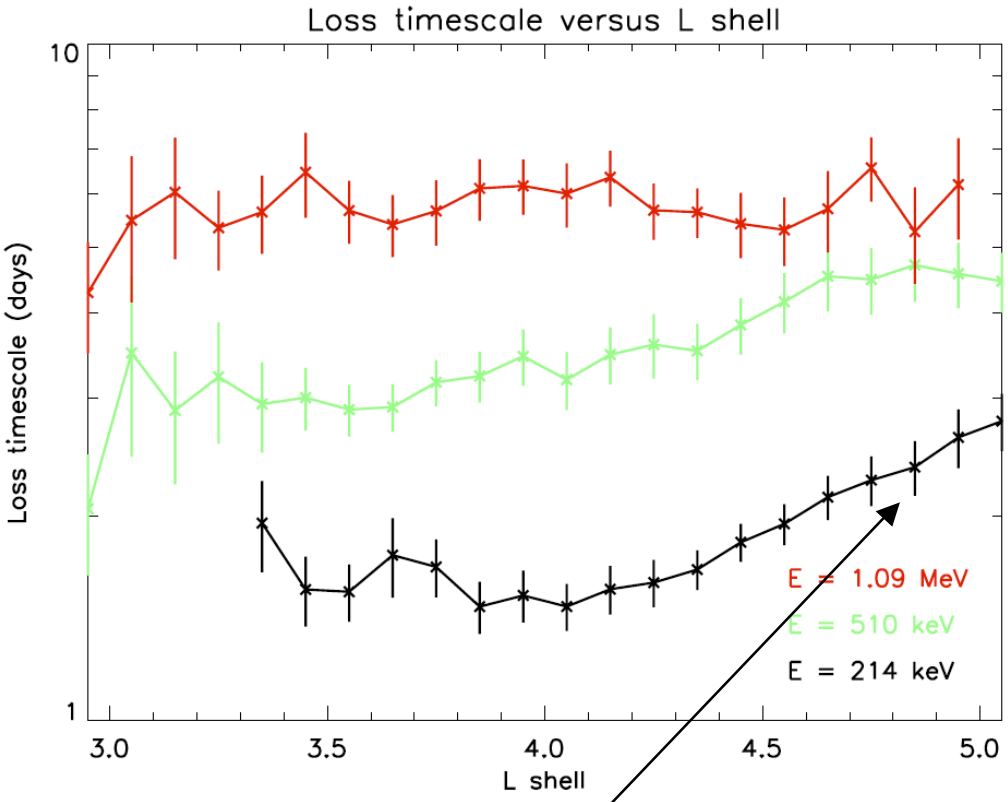

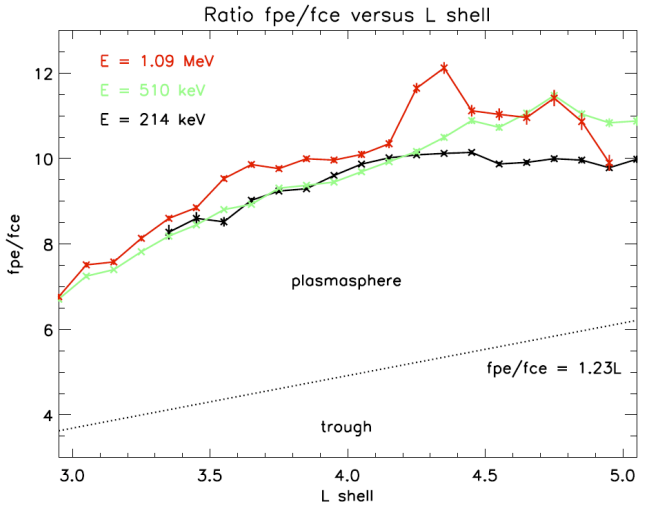

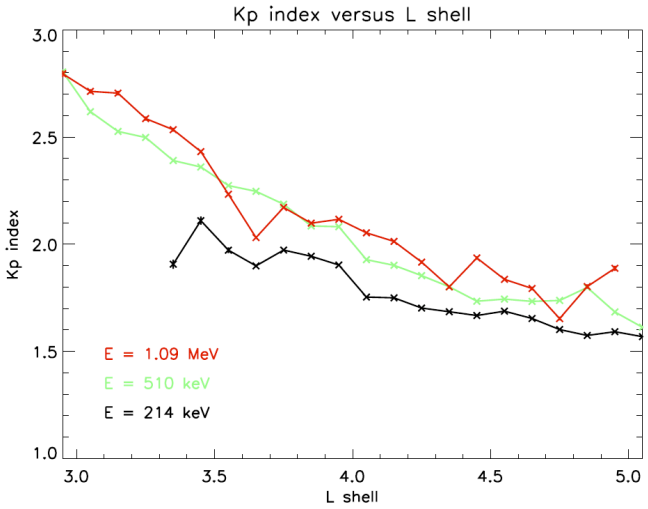

Lower energy decay rates could be affected by convective or diffusive injection in the outer region

Comparison of Decay Rates with QL Scattering by Hiss

Meredith et al., JGR 2005

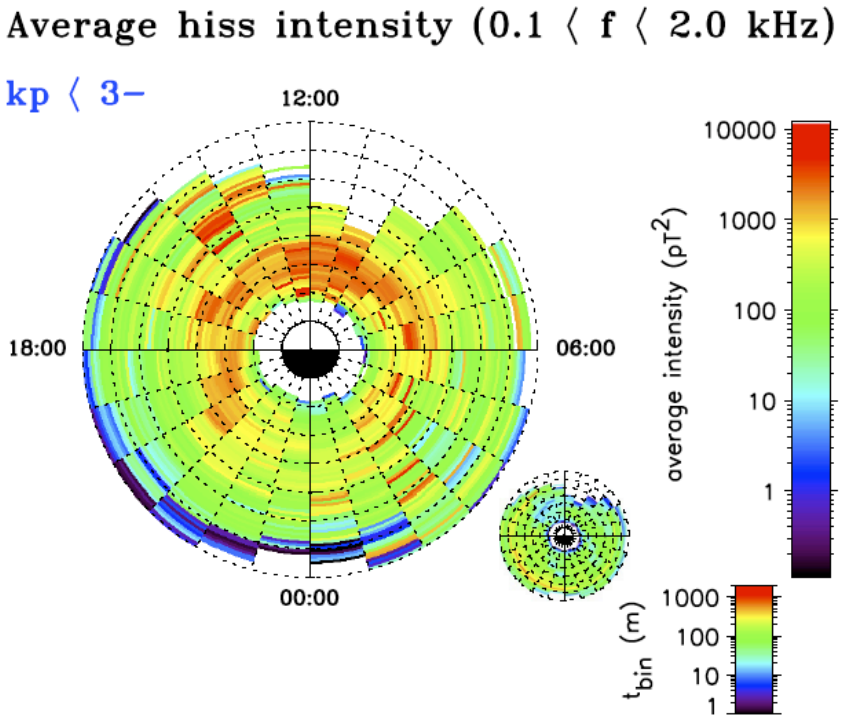

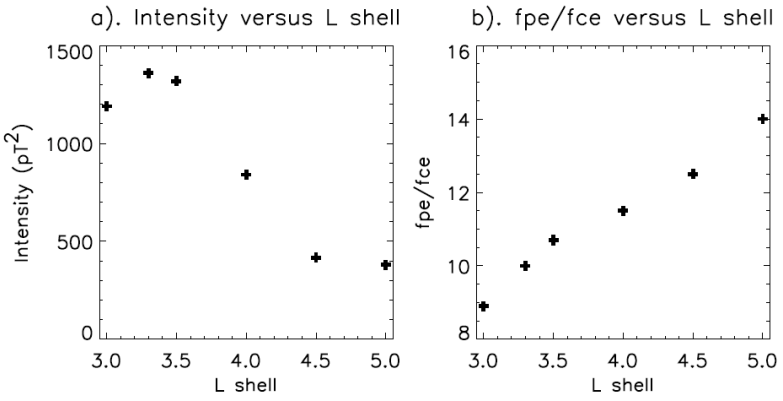

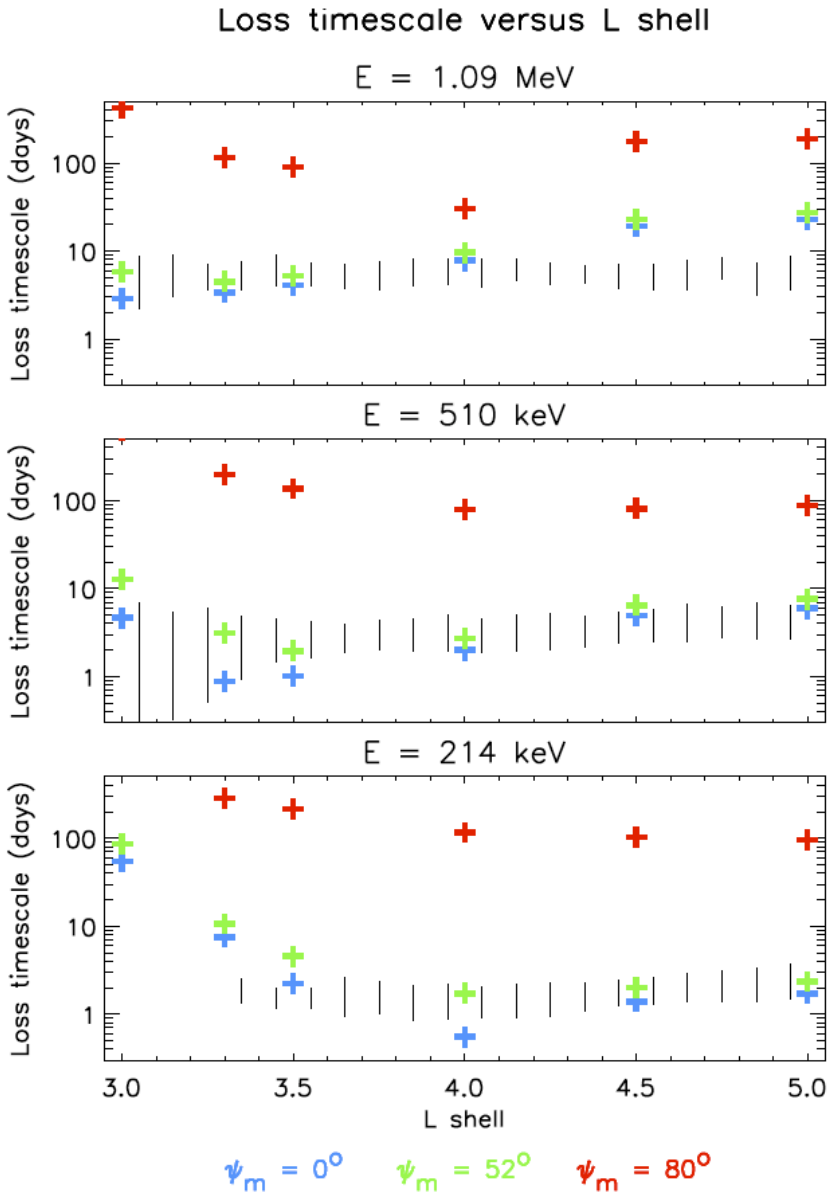

2. Resonant Interactions with Whistler-mode Chorus

$$\omega - k_{ll} v_{ll} = n \Omega_{gyro}/\gamma$$

Landau resonance; n=0
Cyclotron resonance; n=1, 2, 3 etc

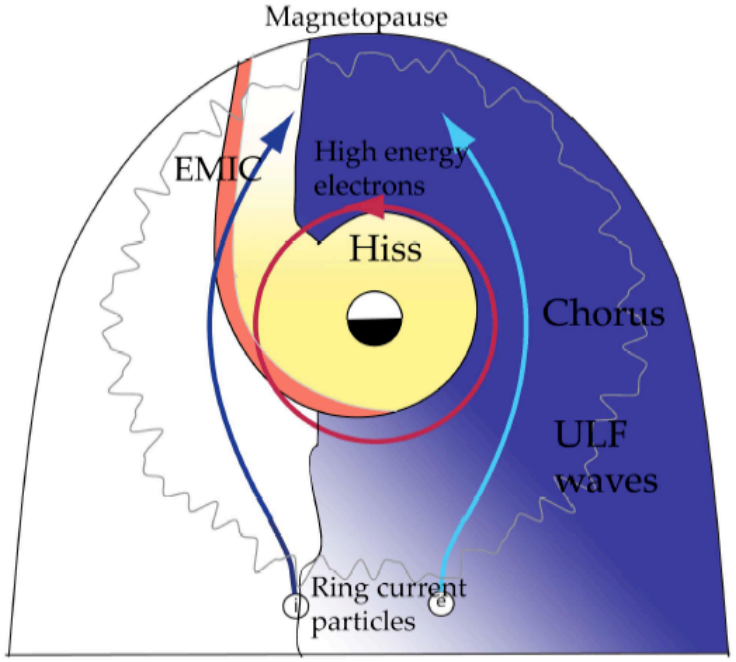

Resonant wave-particle interactions cause both:

(1) pitch-angle scattering (loss to the atmosphere)

(2) Local energy diffusion in the low density region outside the plasmapause

Chorus Properties:

B_{wave} ~ 30-100 pT

$0.2 < \omega/\Omega_e < 0.7$

Strong diffusion at 10 keV

Weak diffusion at 1 MeV

Microburst Precipitation due to Whistler Chorus

Equatorial Lower-Band Chorus and MeV Microbursts, Kp 4-6 O'Brien et al., 2003, 2004

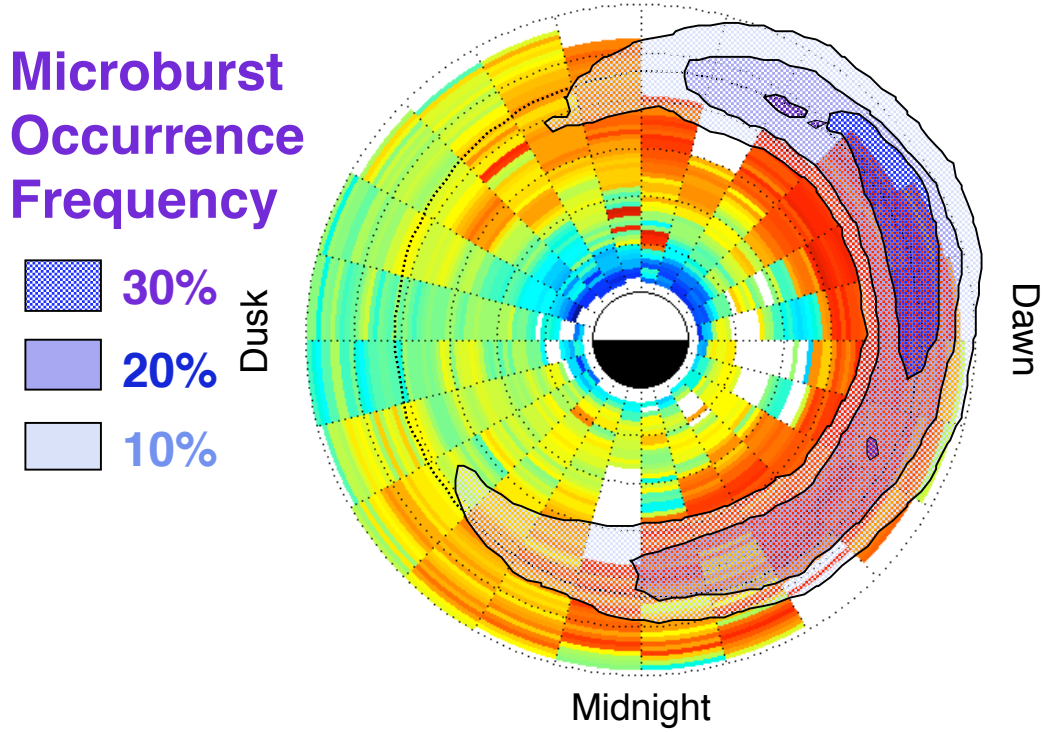

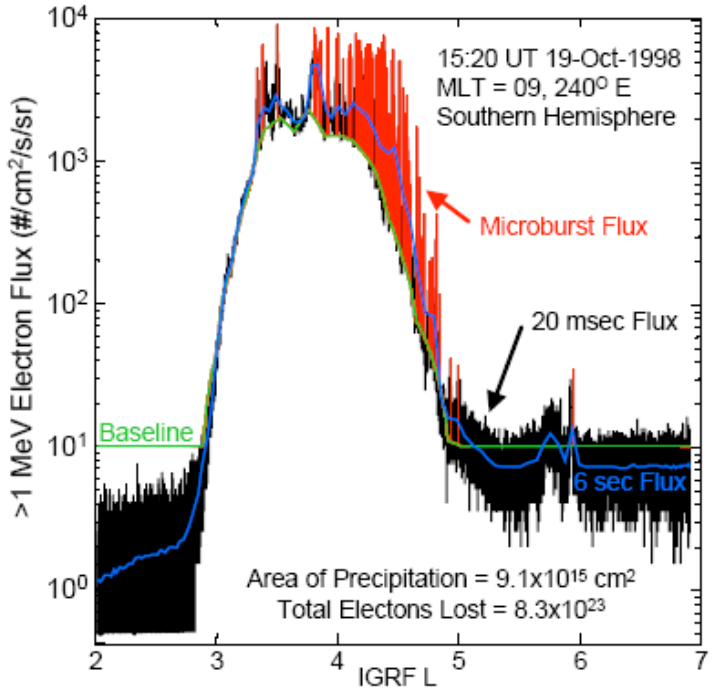

- Chorus and bursty MeV electron precipitation seen by SAMPEX are both observed around dawn [*O'Brien et al.*, 2003; *Nakamura et al.*, 2000; *Lorentzen et al.*, 2000] .
- Chorus risers and microbursts last for the same time and individual chorus risers from Polar have been correlated with microbursts observed at low altitude by SAMPEX [*Lorentzen et al.*, 2000].

Microbursts Loss Maximizes During Storm Main Phase

O'Brien et al., 2004

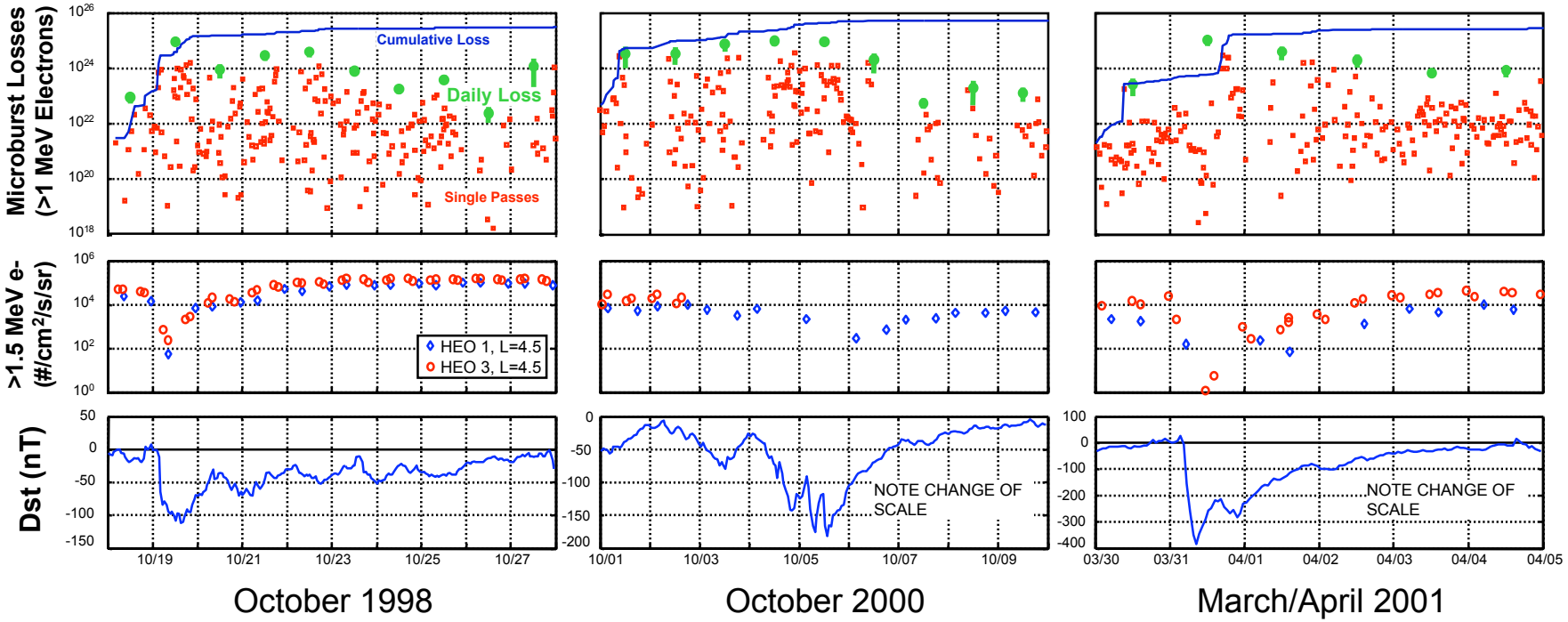

- Main phase microburst losses (~10^{25} electrons) empty the radiation belts of >1 MeV electrons over a day
- Although microbursts continue during the recovery phase, the net loss rates are much lower (many days, QL :Horne et al., 2005)
- Microbursts are a loss process that can also be used as a proxy for electron acceleration [O'Brien et al., 2003]

Analysis of Electron Lifetimes due to Microburst Precipitation

Thorne et al., JGR, 2005

Comparison between precipitation flux observed on SAMPEX and trapped flux on POLAR during the main phase of the October 1998 storm yield lifetimes comparable to a day. This agrees with theoretical calculations of diffusion rates.

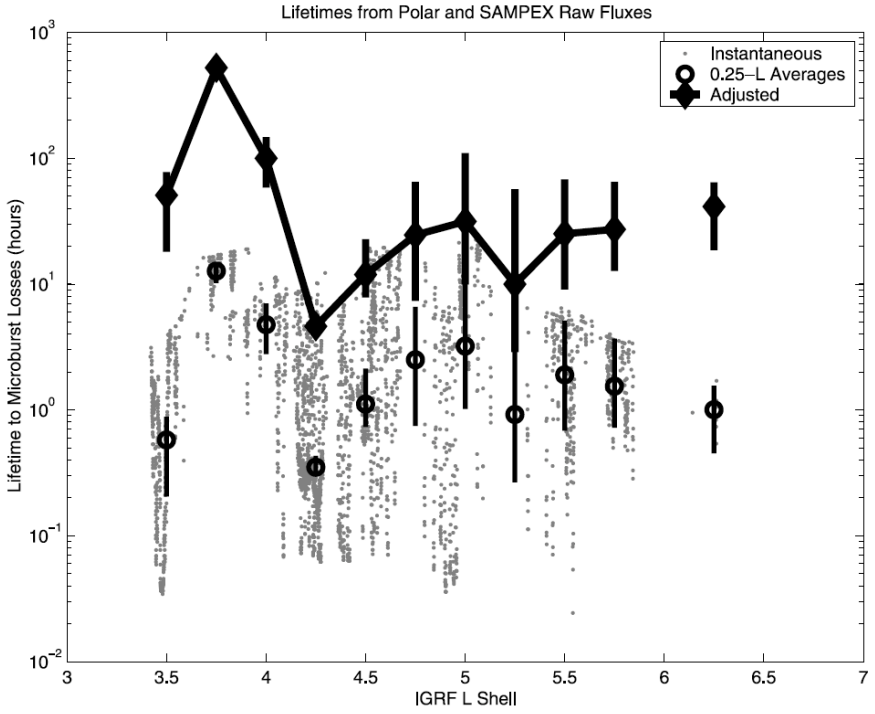

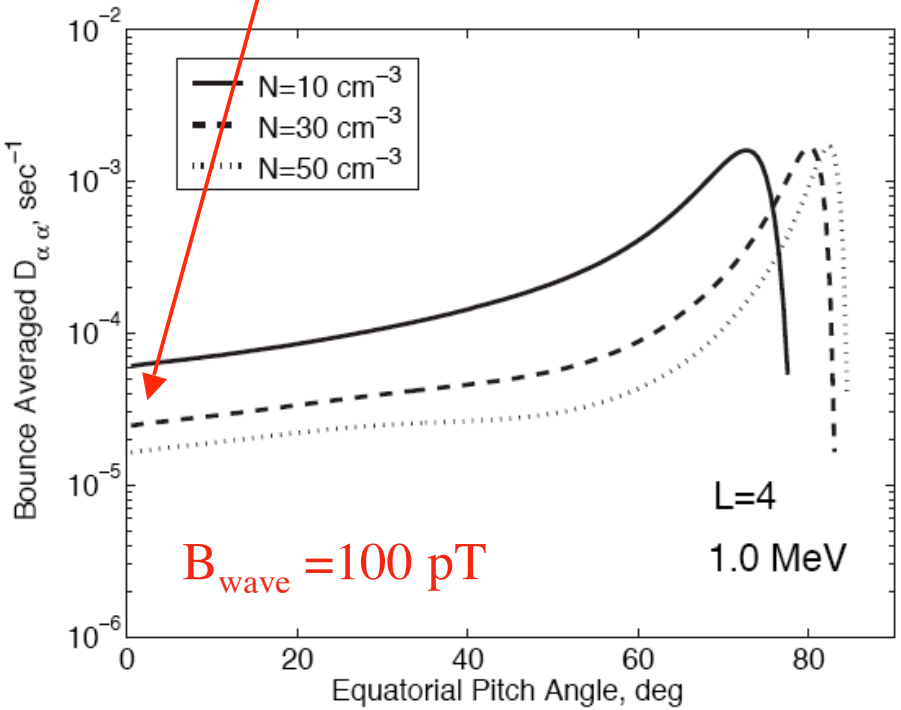

Sudden Electron Loss During Storm Main Phase

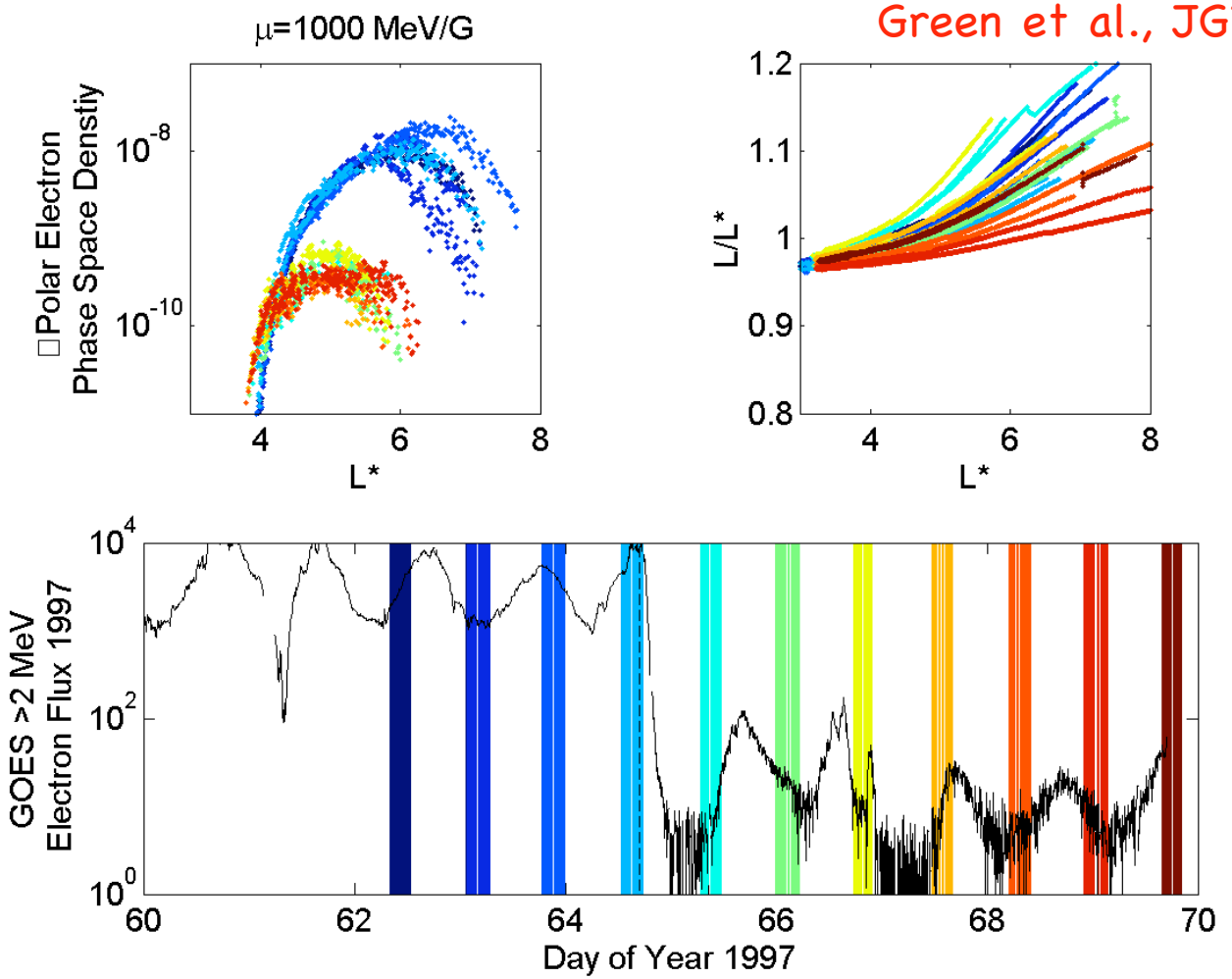

Polar observes loss down to L^*=4. It is unlikely that adiabatic motion pushes electrons from L^*=4 to the magnetopause boundary. What is the loss process?

3. Resonant Wave-Particle Interactions with EMIC Waves

$$\omega - k_{ll} v_{ll} = n \Omega_{gyro}/\gamma$$

Landau resonance; n=0
Cyclotron resonance; n=1, 2, 3 etc

*Resonant interactions with EMIC waves cause pitch-angle scattering (loss to the atmosphere).

*Electrons must overtake the L-mode waves and minimum resonant energies are comparable to an MeV.

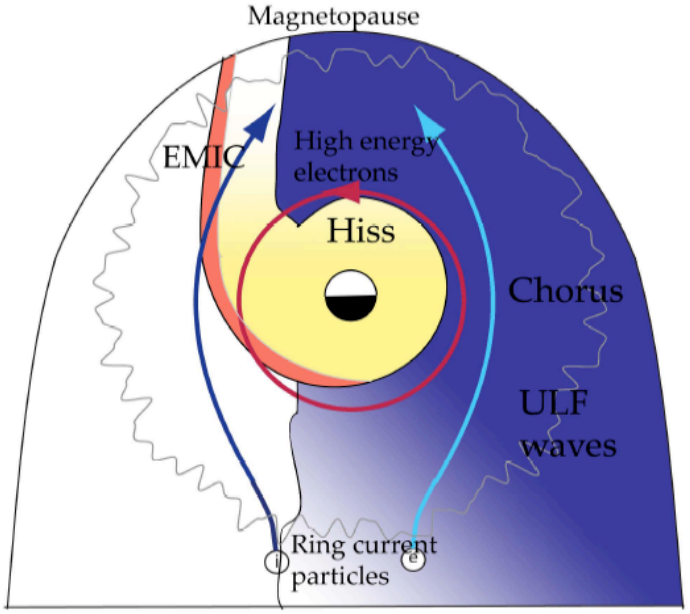

EMIC Properties:

B_{wave} ~ 1-10 nT

ω/Ω_e < 1/2000

Strong diffusion scattering of ring current ions and > 1 MeV electrons

EMIC Waves Observed on CRRES Within a Plume

Intense (few nT) EMIC waves observed near 1600 MLT between L = 4.5-6.

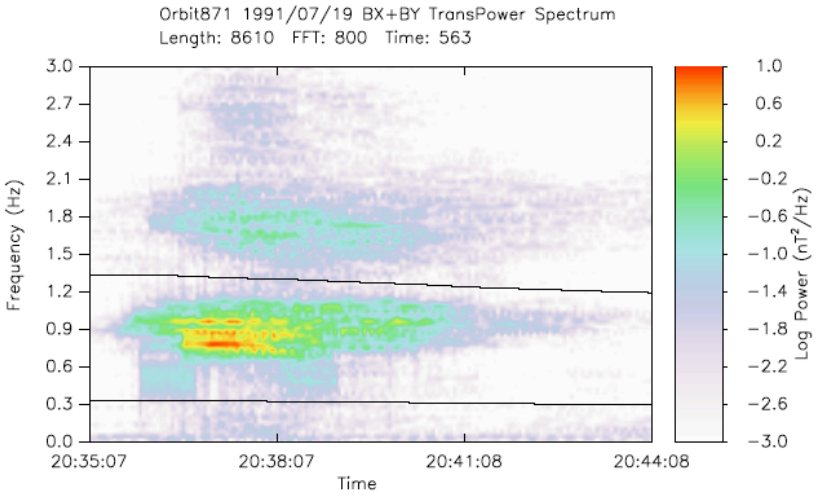

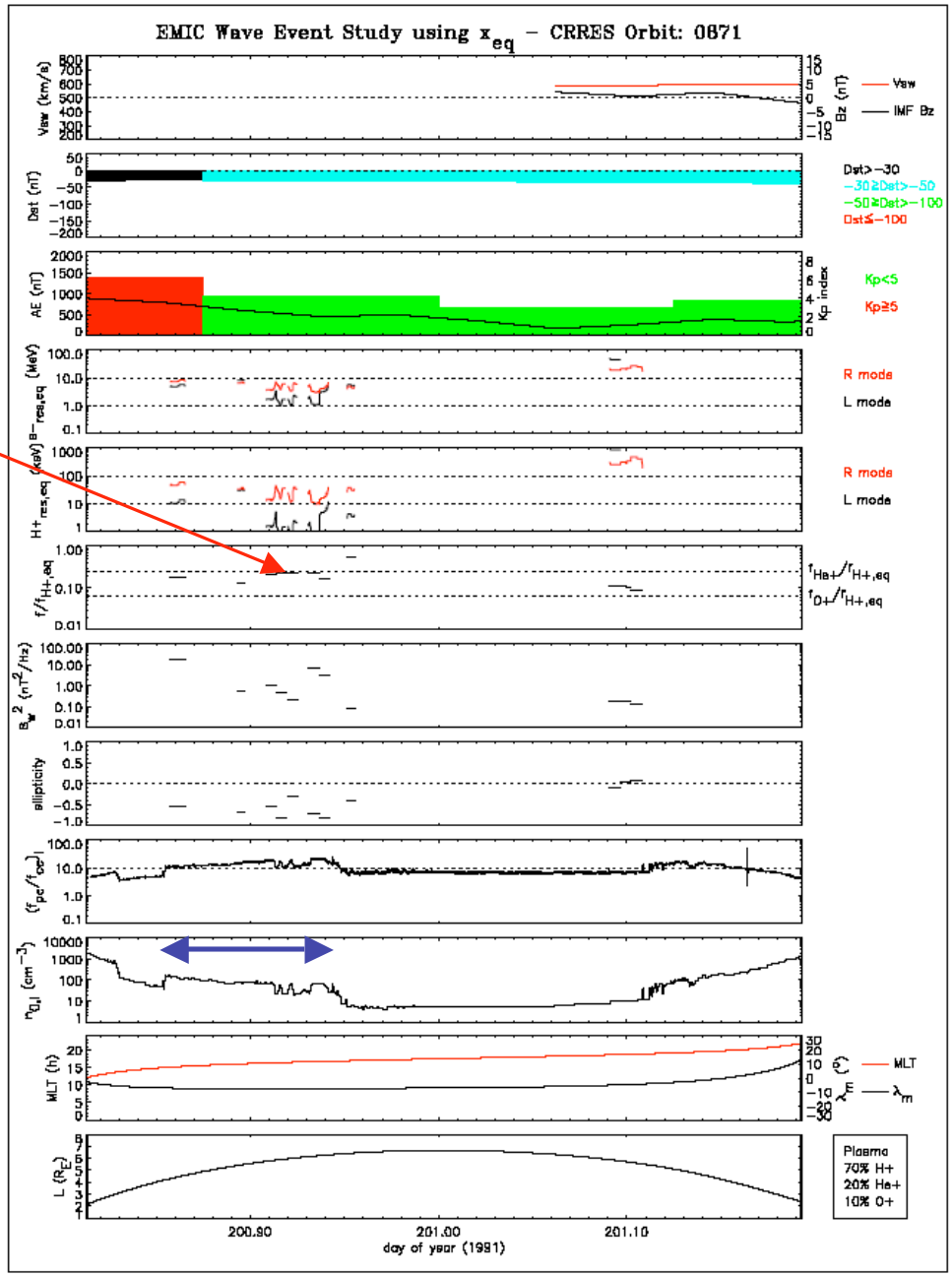

Resonant Electron Energy for Scattering by EMIC Waves

$$\omega - kv_{\parallel} = N|\Omega_e|/\gamma$$

Resonant electron energies minimize for wave frequencies just below each ion gyrofrequency.

Resonant energies are also lower in high density regions (just inside the plasmapause or within drainage plumes)

$$\alpha^* = \frac{\Omega_e^2}{\omega_{pe}^2} = \frac{1}{\epsilon}\frac{V_A^2}{c^2} = \frac{B_0^2}{4\pi N_0}\cdot\frac{1}{m_e c^2},$$

Summers and Thorne, JGR 2003

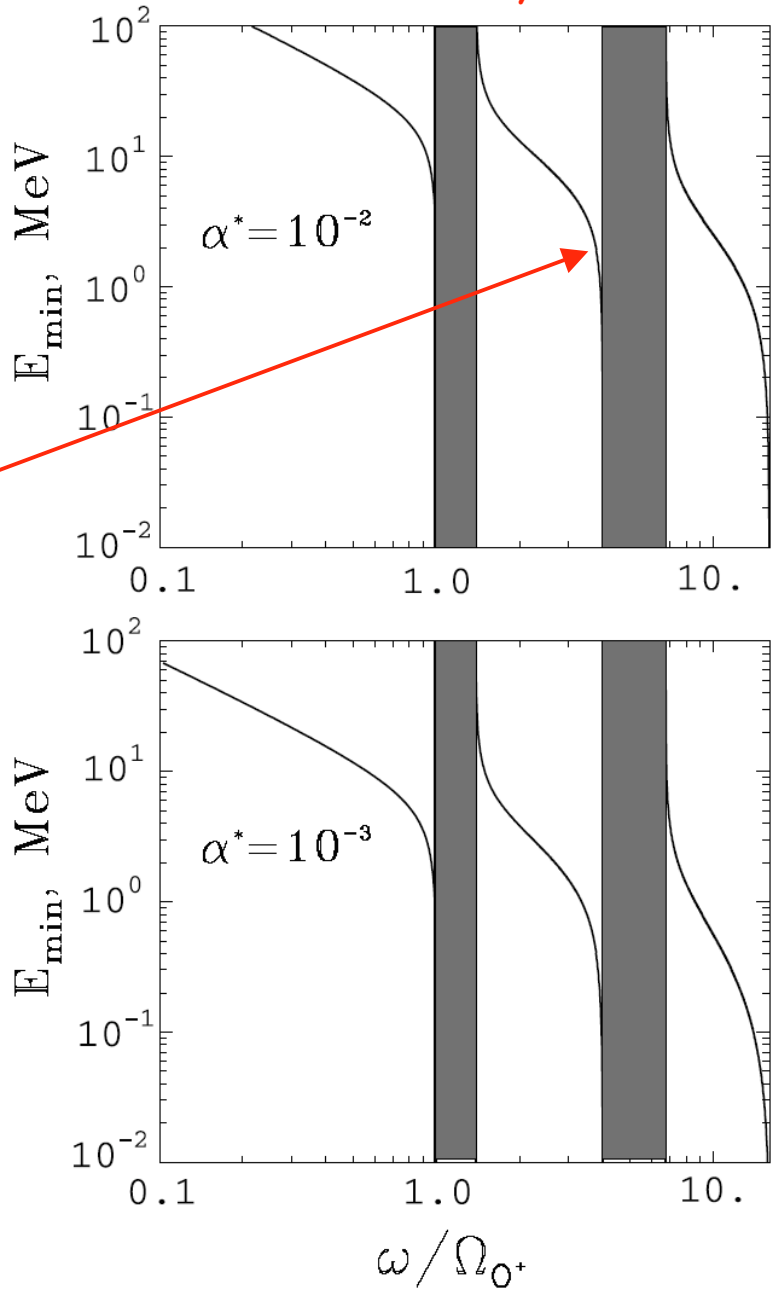

Could EMIC Wave Scattering Account for Main Phase Loss?

Paul O'Brien

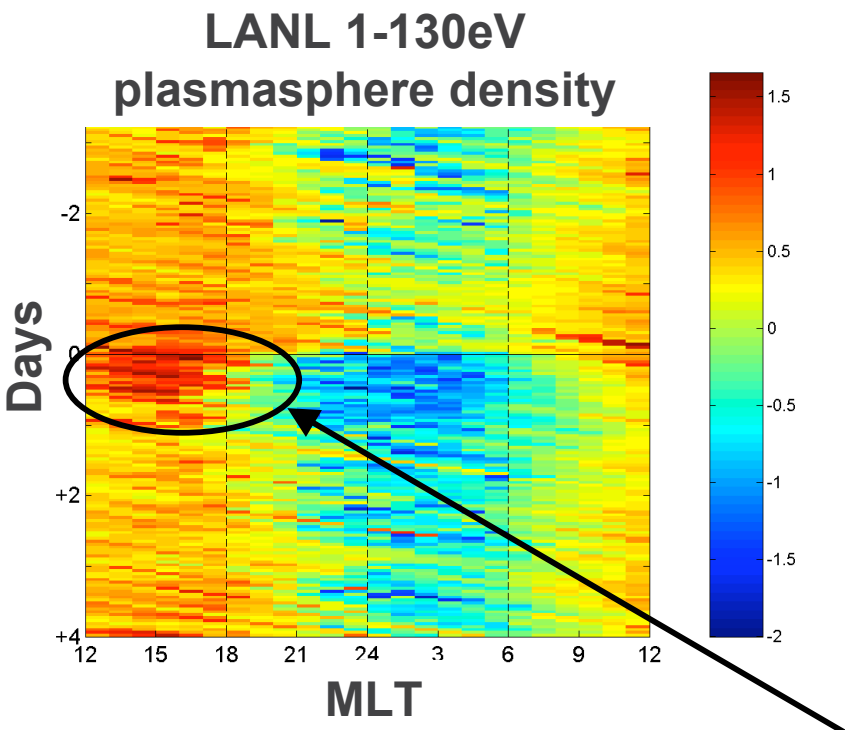

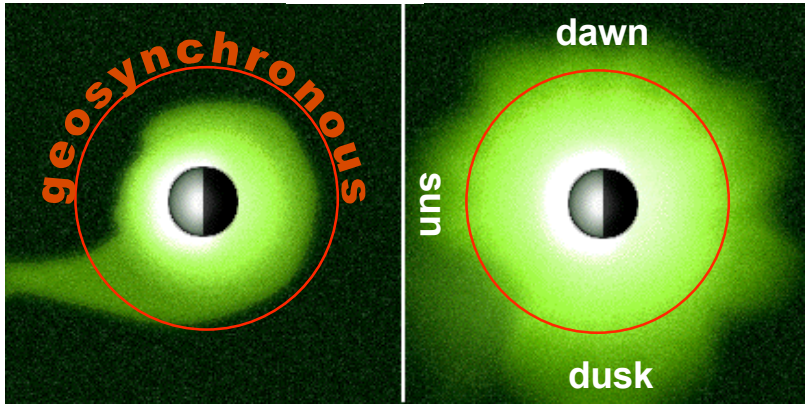

Plasmasphere schematic

- EMIC waves scatter electrons at a resonant energy which depends on the magnetic magnitude and plasma density. High density is needed for these waves to scatter MeV electrons.
- High density plumes are indeed observed during the first day of the events from 12-18 MLT Green et al., [2004].

EMIC Wave Excitation and Subauroral Proton Arcs

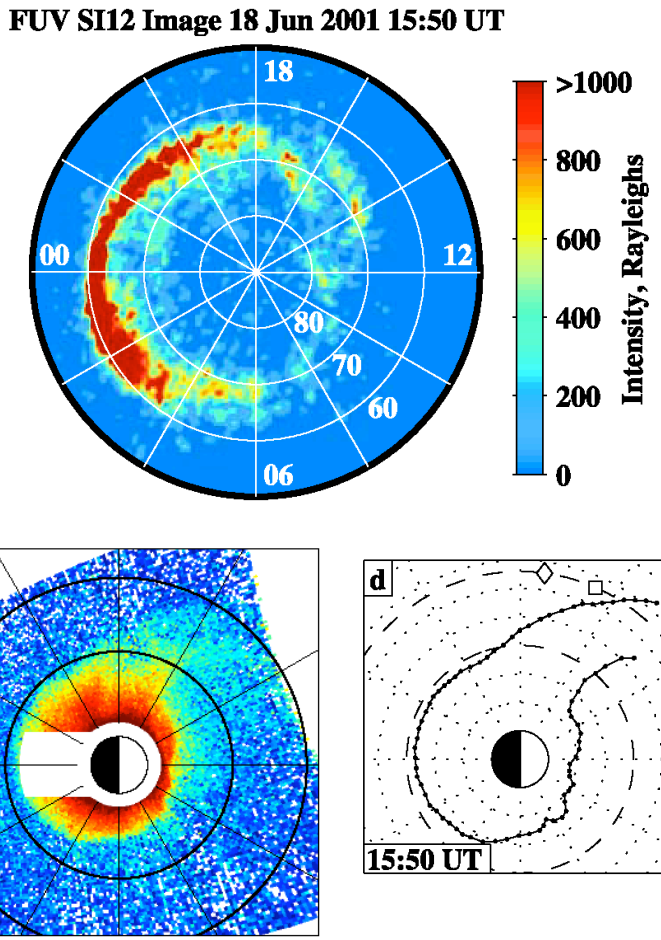

Direct link between a subauroral arc and a global observation of a plasmaspheric plume by IMAGE [Spasojevic et al., 2004]

RAM simulations: June 17-18, 2001

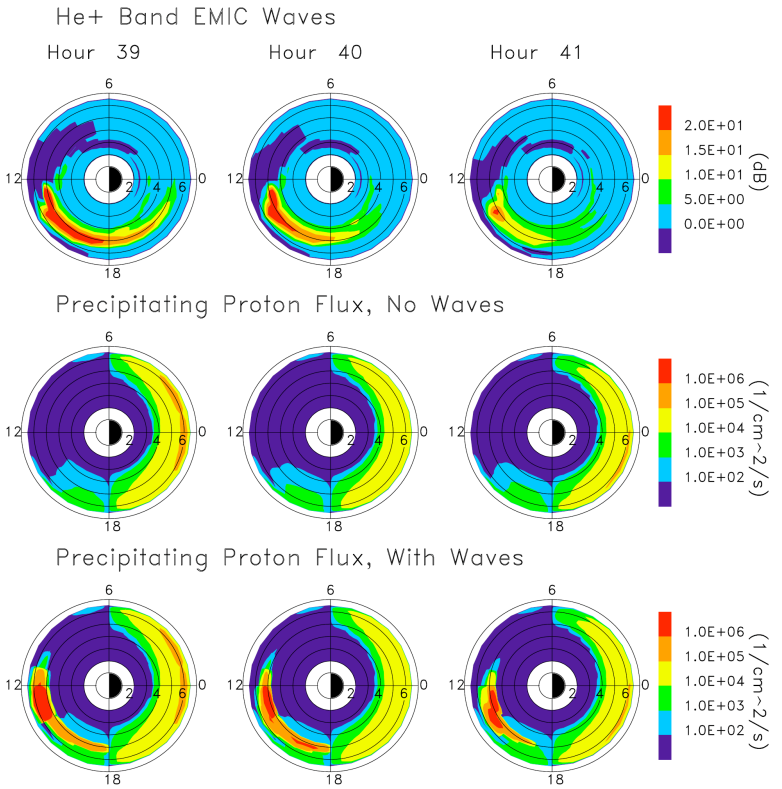

Hours after 00 UT, April 17, 2001

EMIC waves are excited near hours 37- 40 in the afternoon MLT sector causing intense ion precipitation [Jordanova et al., 2006]

Ion and Electron Scattering Rates Obtained by the PADIE Code

Assuming a Gaussian distribution of EMIC waves between 2.2-3.8 Ω_o with B_w= 1nT

Ion scattering leading to sub-auroral arcs

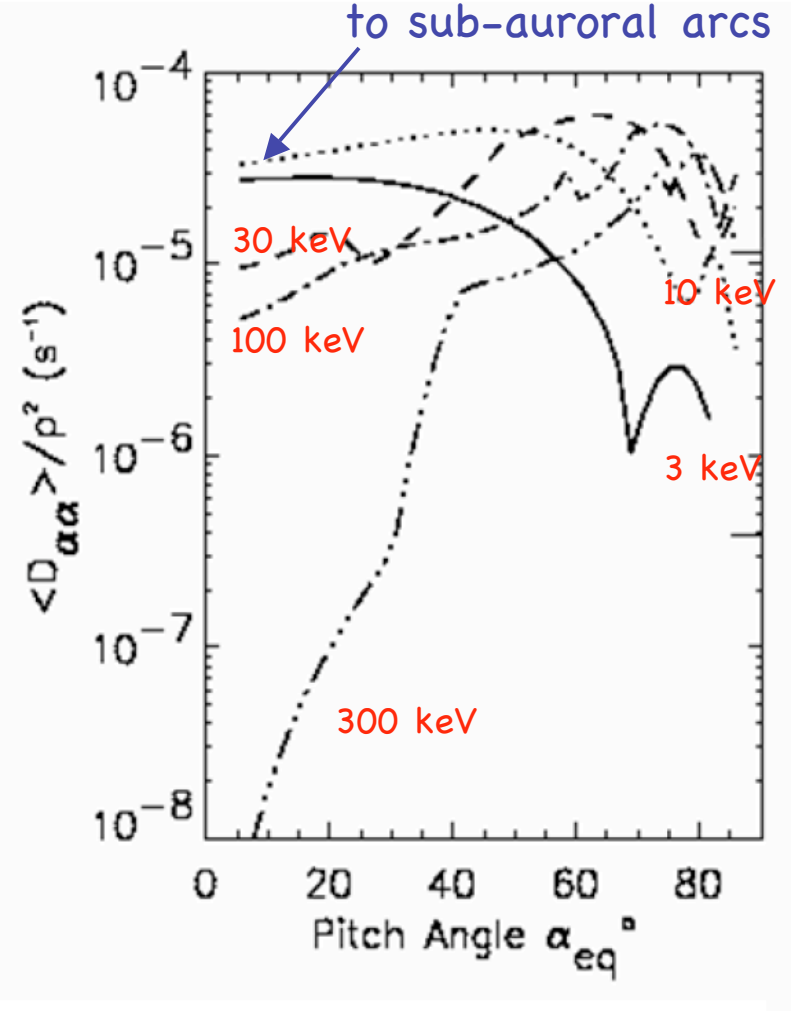

Rapid relativistic electron scattering above 1 MeV

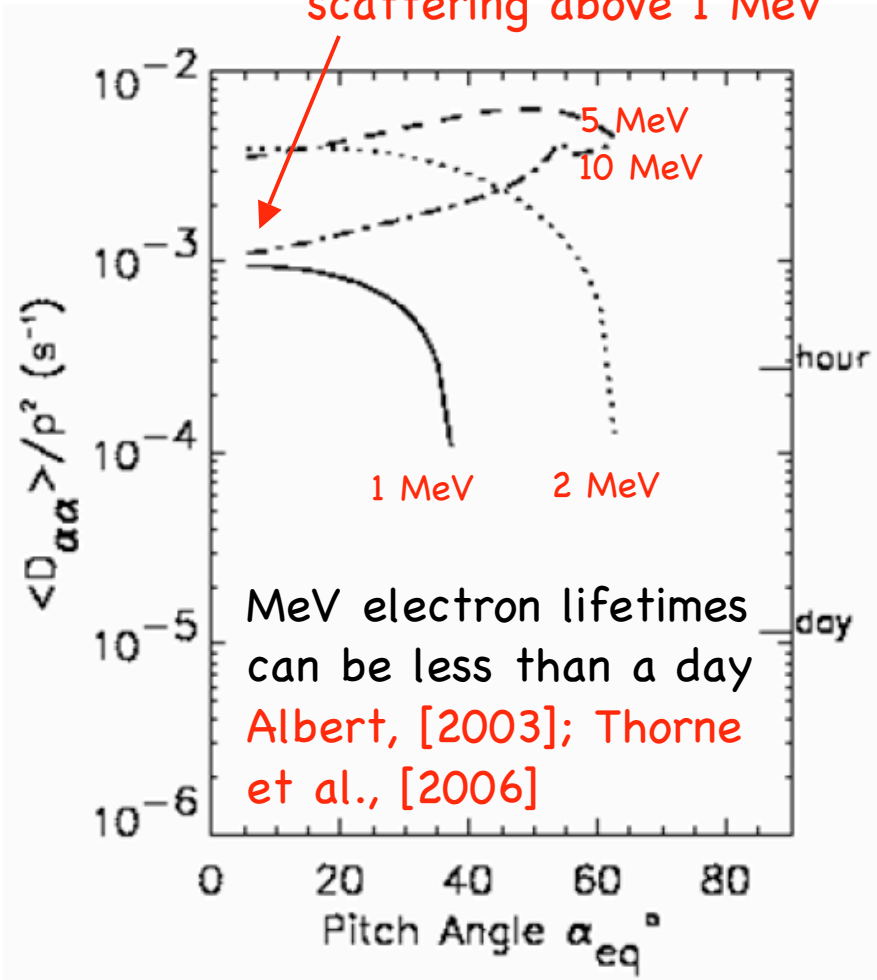

MeV electron lifetimes can be less than a day Albert, [2003]; Thorne et al., [2006]

Evidence for Electron Precipitation Loss by EMIC Waves

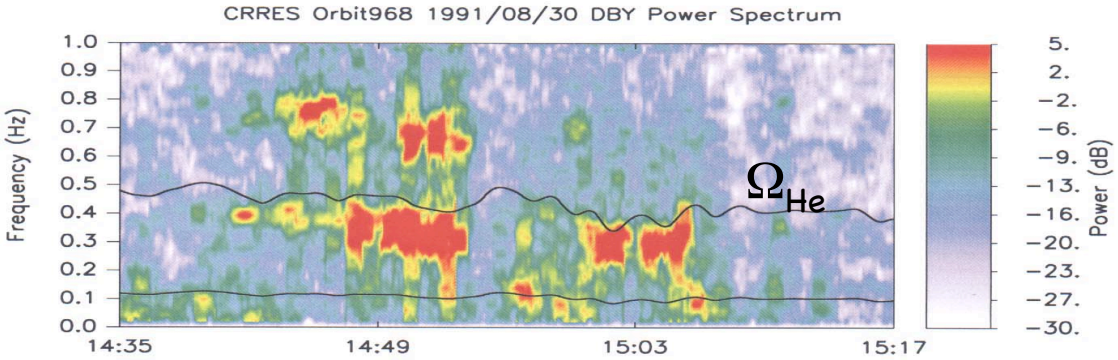

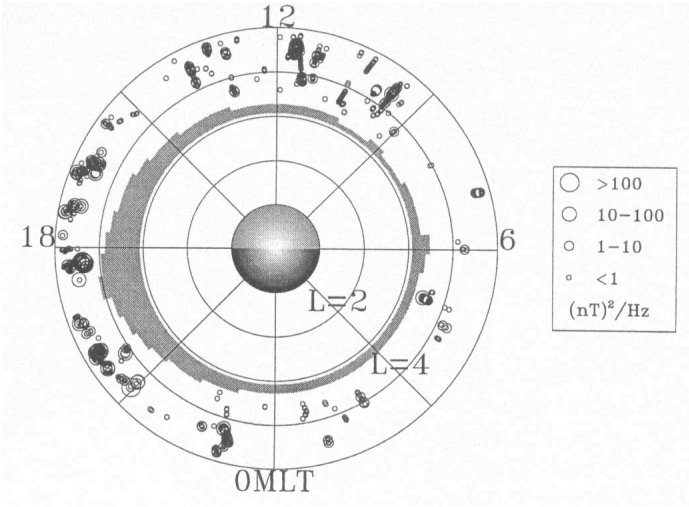

Statistics of EMIC waves observed on DE

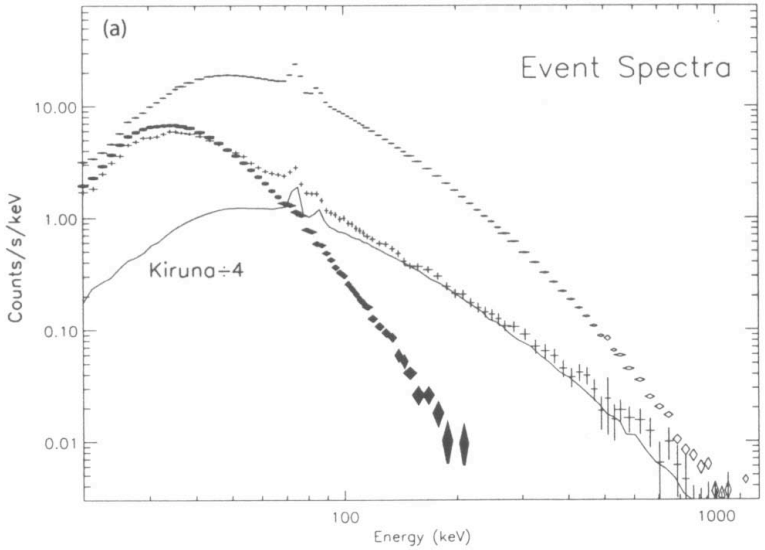

Extremely hard X-ray events observed on balloons: Millan et al., GRL 2002

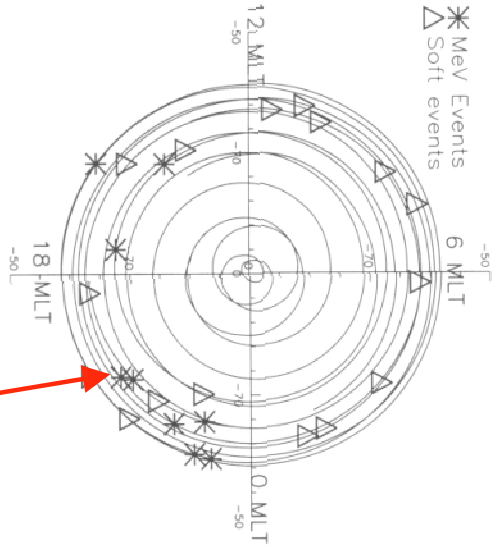

January 19, 2000 Event

Robyn Millan

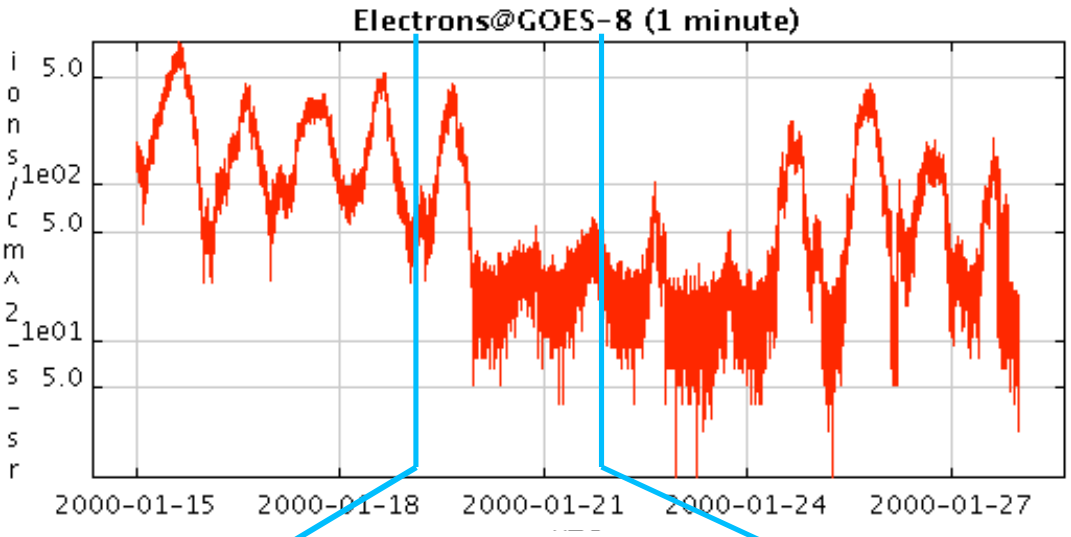

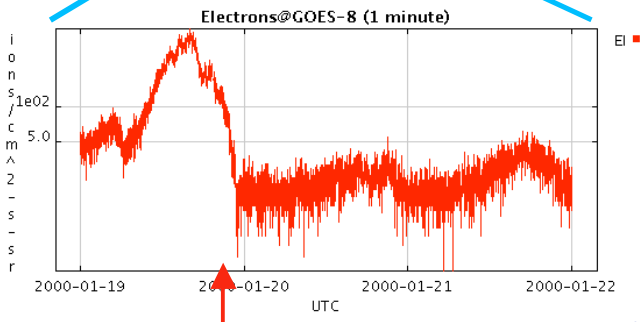

X-ray burst

- X-ray burst on Jan. 19, 2000 occurred during a flux dropout as seen by GOES-8 and GOES-10.

MAXIS Observations on Jan. 19. 2000

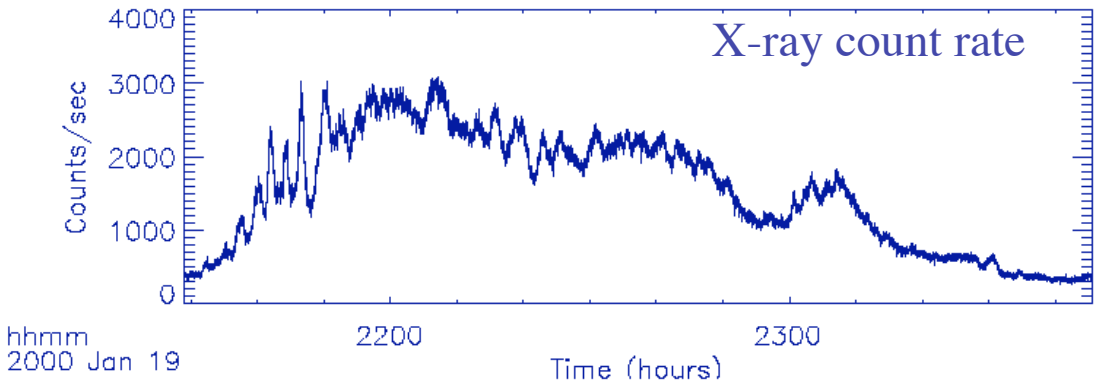

Reduction in Trapped Electron Flux Observed on HEO During a Large Magnetic Storm on November 20, 2003;

Bortnik et al. 2006

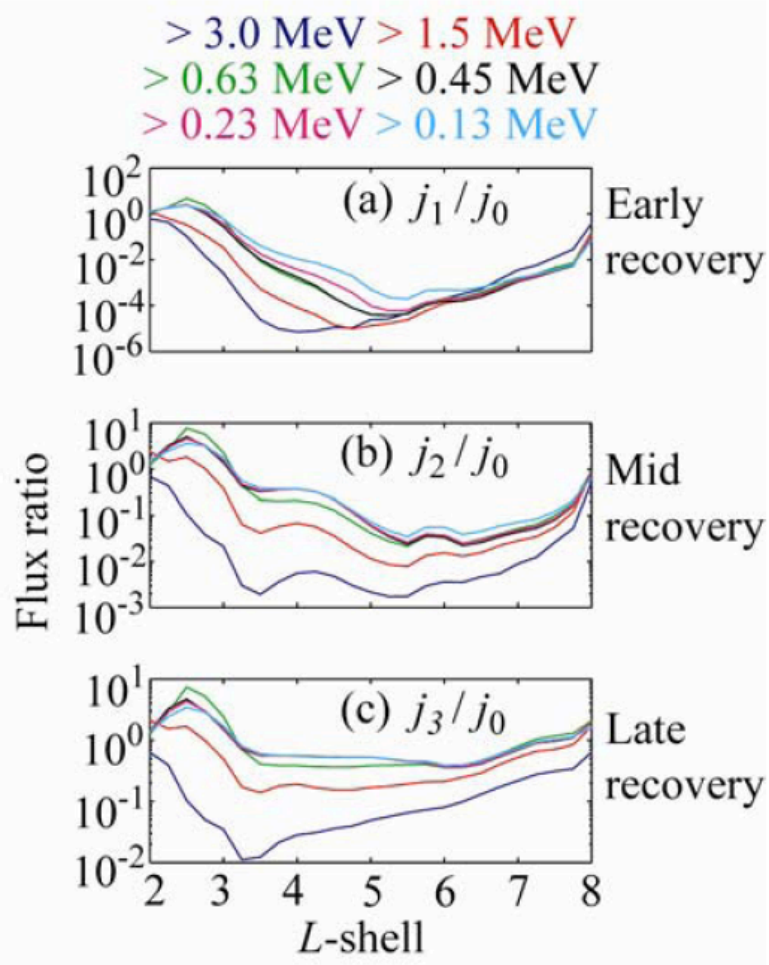

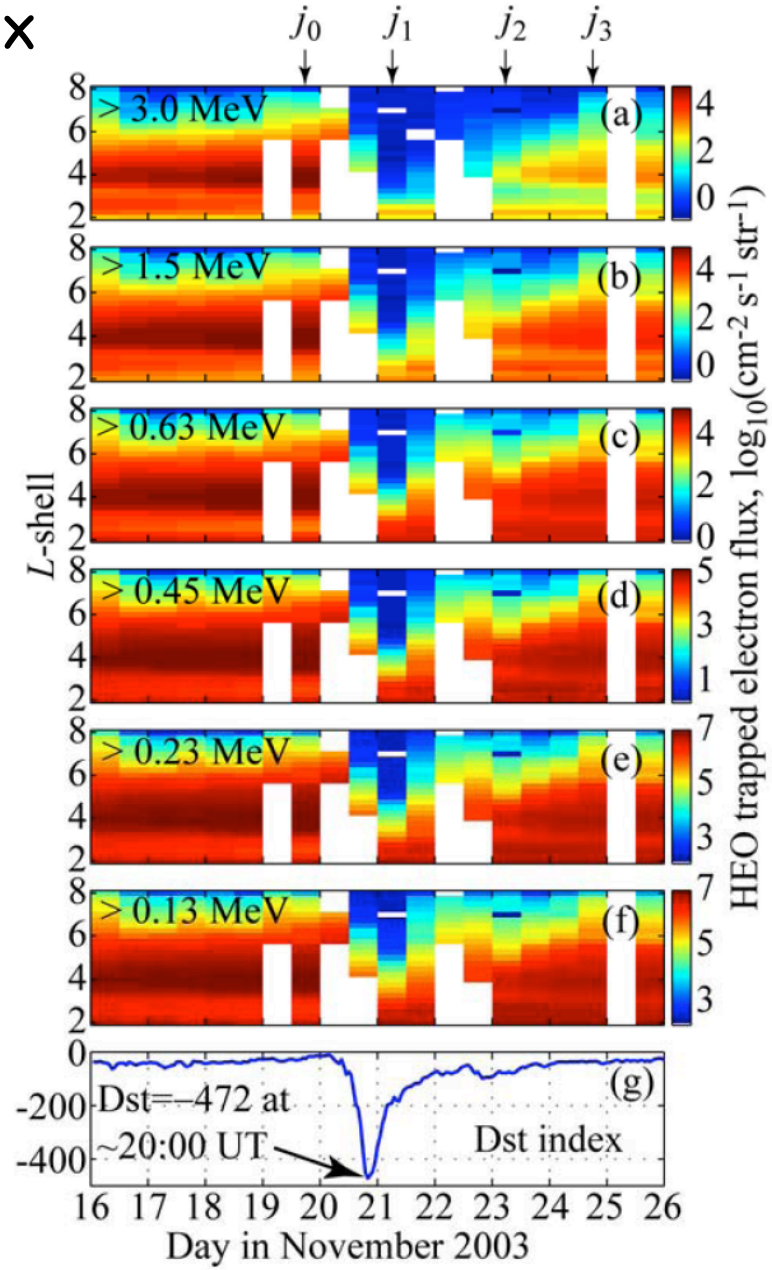

Location of SAMPEX Electron Precipitation Bands in Relation to Trapped Flux and the Plasmapause and Magnetopause Boundary

Bortnik et al. 2006

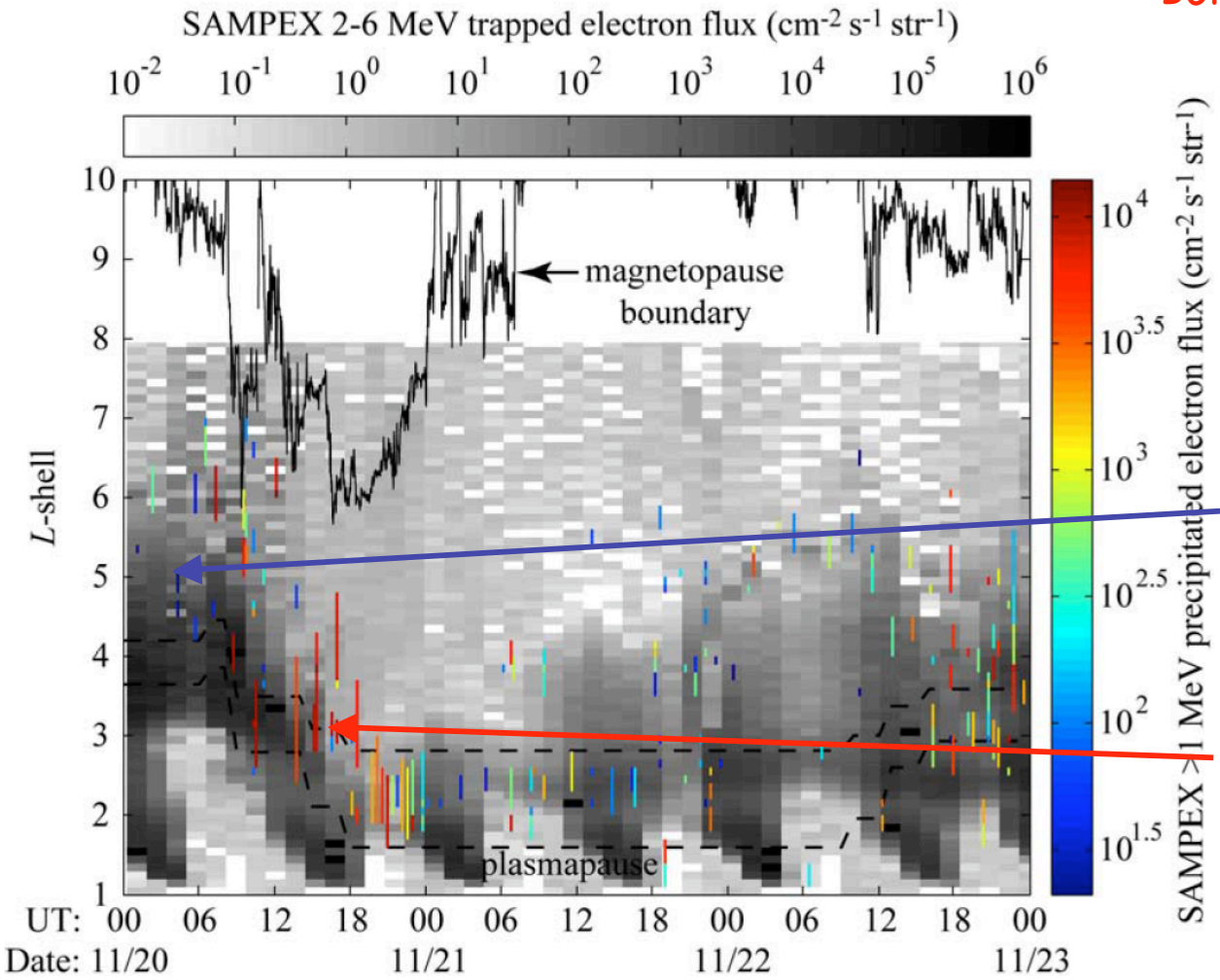

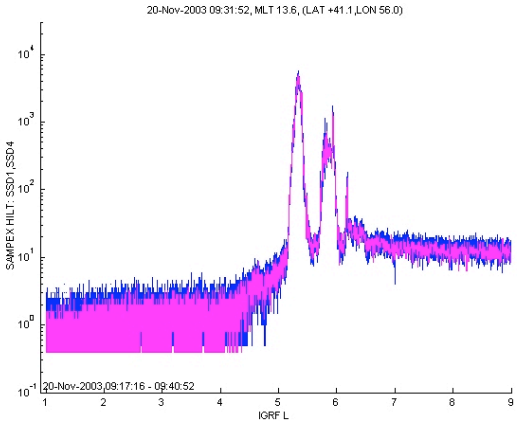

Precipitation at L>5 prior to storm onset

Scattering by EMIC waves along the stormtime Plasmapause between L=2-4 as storm intensifies could explain HEO loss at E < 0.5 MeV

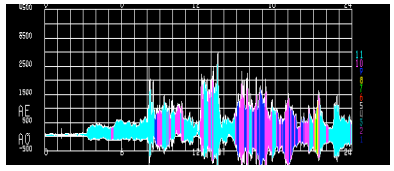

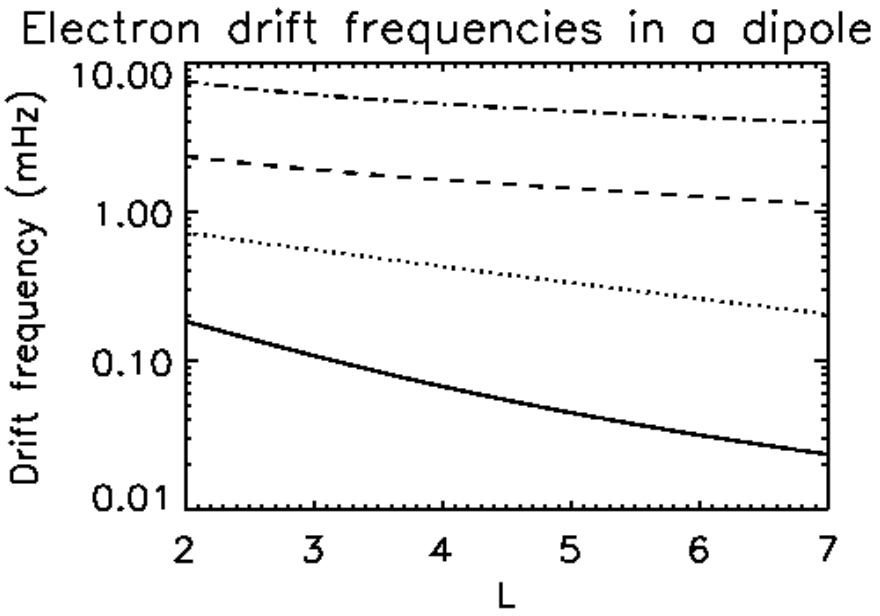

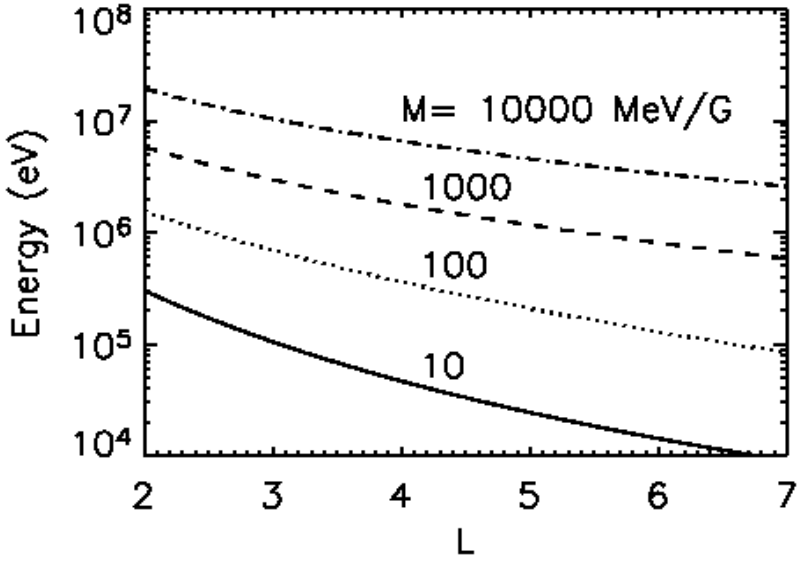

Drift Resonance With ULF Waves

- Drift resonance when wave frequency matches the particle drift frequency
- Toroidal and poloidal modes m=2
- For E~ 1 - 5 MeV at L ~ 4
  - Need waves at ~ 0.2 - few mHz
- 1st and 2nd adiabatic invariants conserved
- Spectrum for different L?
- Frequency bandwidth?
- MLT occurrence?

External Sources of Magnetospheric Energy at ULF Frequencies

Scot Elkington

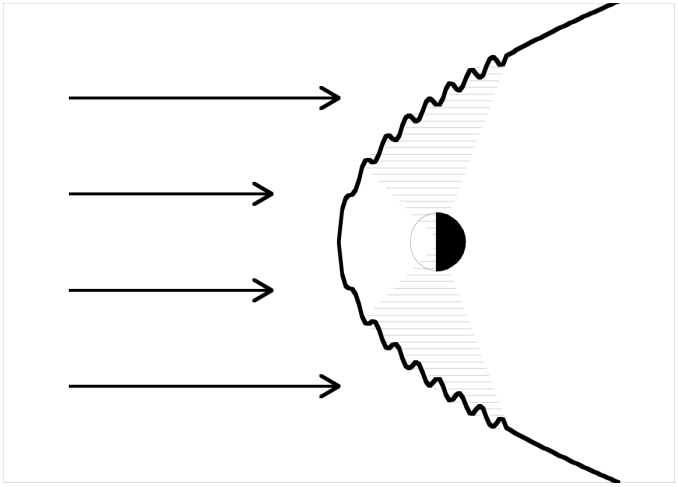

Shear waves on the flanks

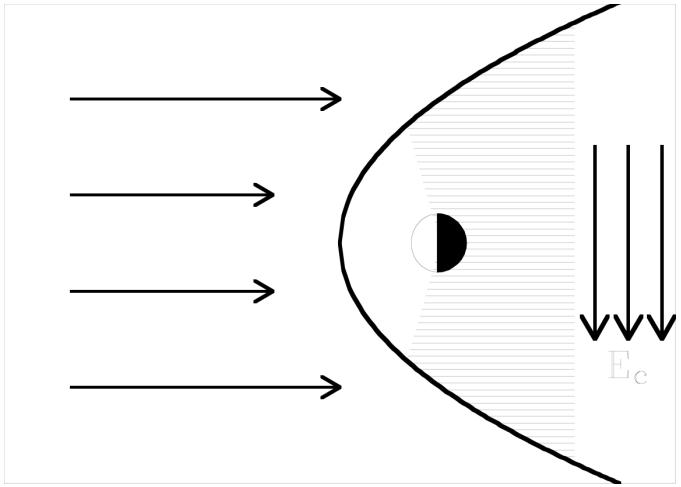

Variations in the convection electric field

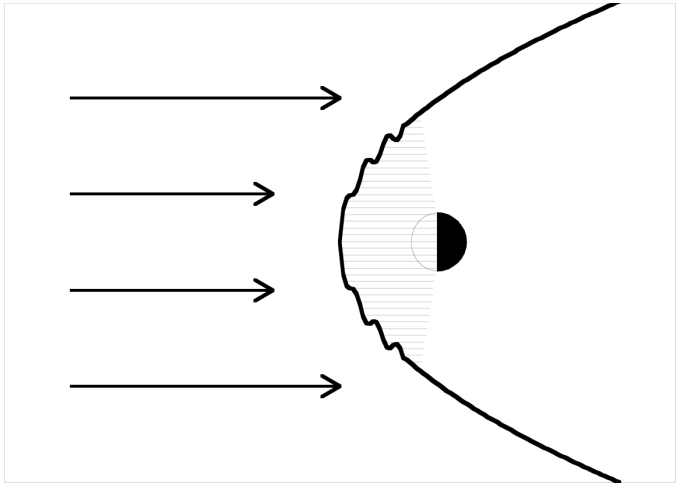

Impulsive variations in the solar wind

Toroidal and Polodial ULF Modes

Mode Structure

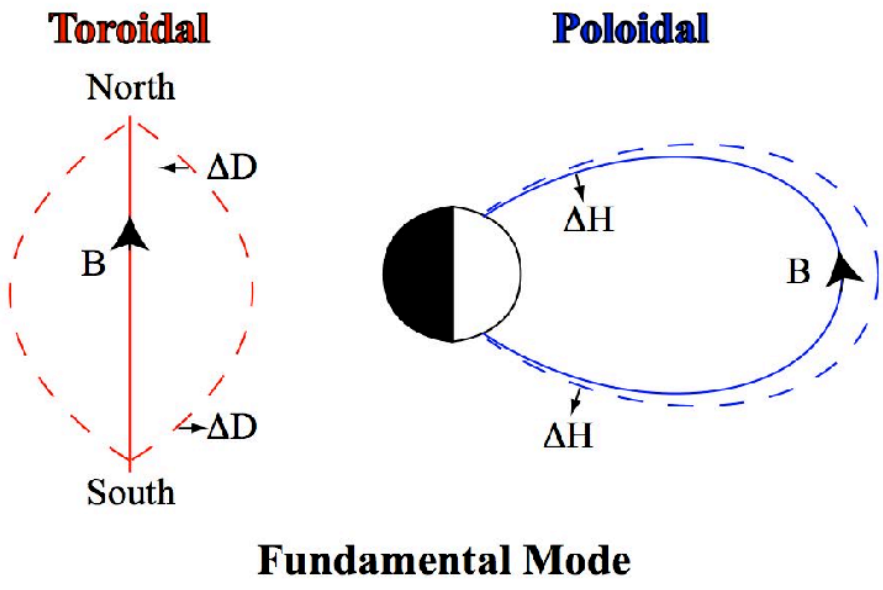

Drift Resonance

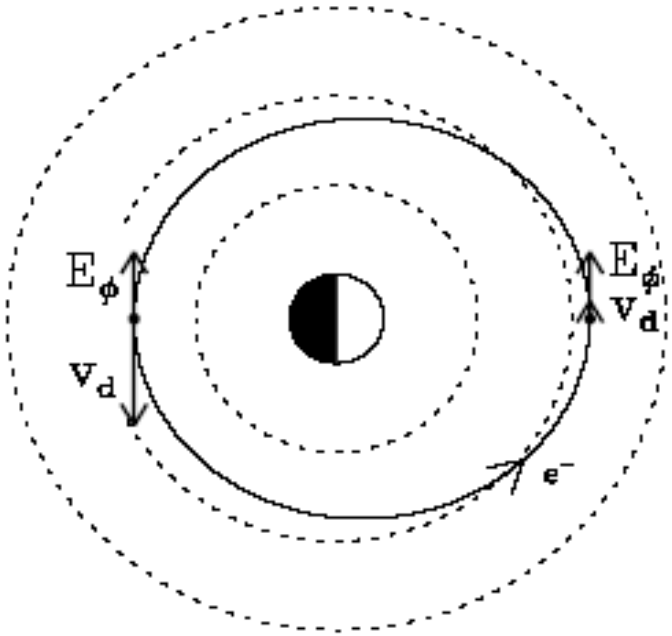

Hughes, *Solar Wind Sources of Magnetospheric ULF Waves*, AGU, 1994

MHD simulations of ULF power, 09/24/1998

Scot Elkington

- ULF power in MHD shows more power at high *L*, low *f*.

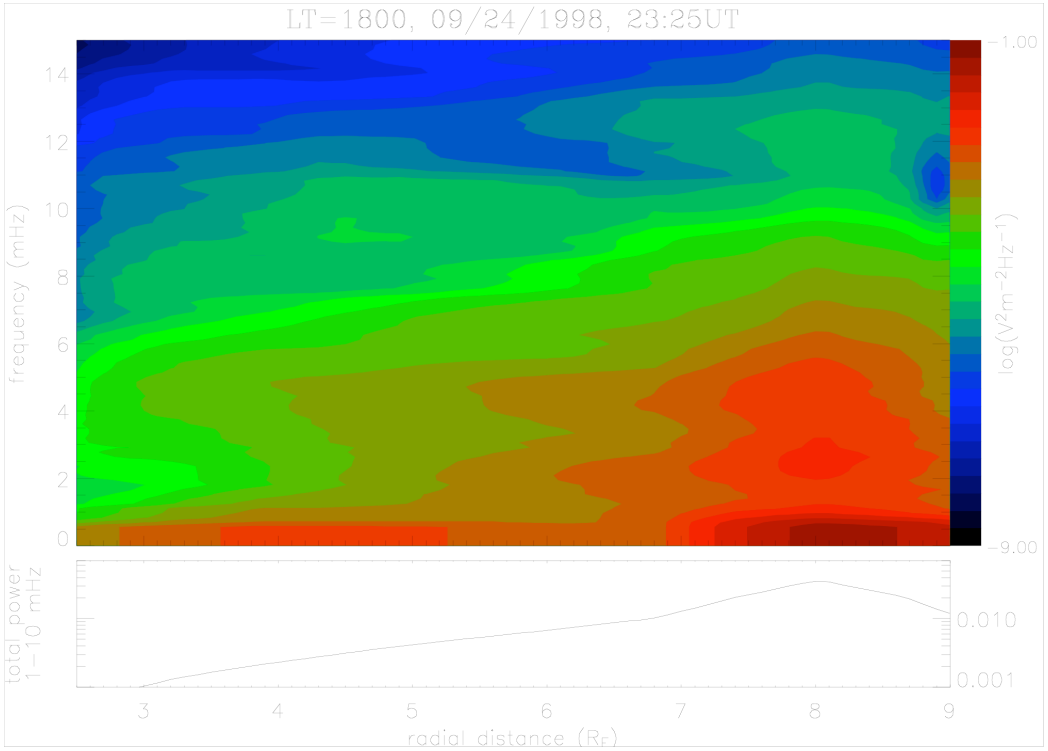

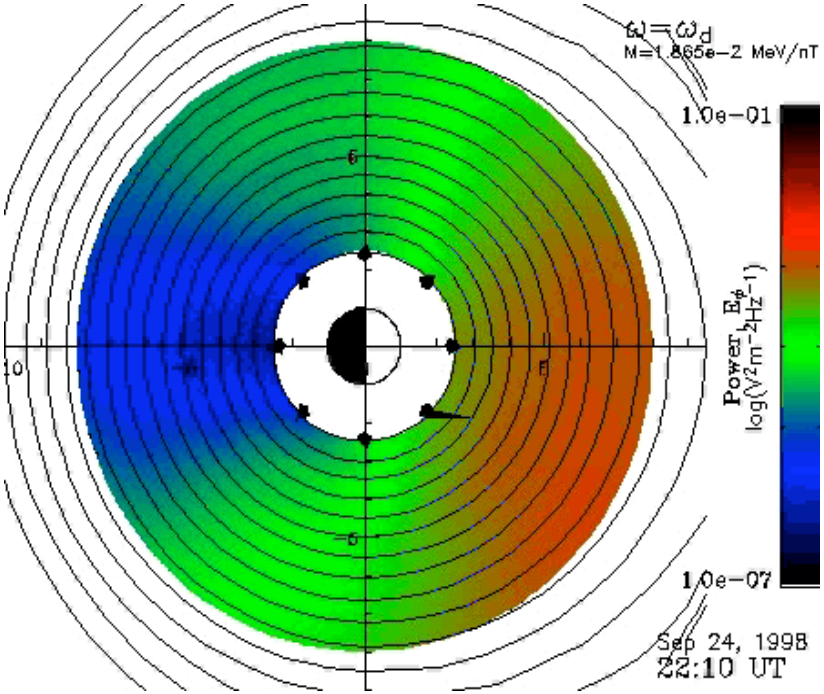

- Azimuthal dependence: structure in local time, mode structure via Holzworth & Mozer [JGR, 1979]

Test Particle Simulations of Radial Diffusion

Scot Elkington

Scenario:

- Ensemble of particles initially at *L*=5 in a dipole field.
- Dynamic waves: analytic ULF with frequencies ~f_d and random phases induce radial diffusion.

Quantifying diffusion:

$$D_{LL} = \frac{\left\langle (\Delta L)^2 \right\rangle}{2\tau}$$

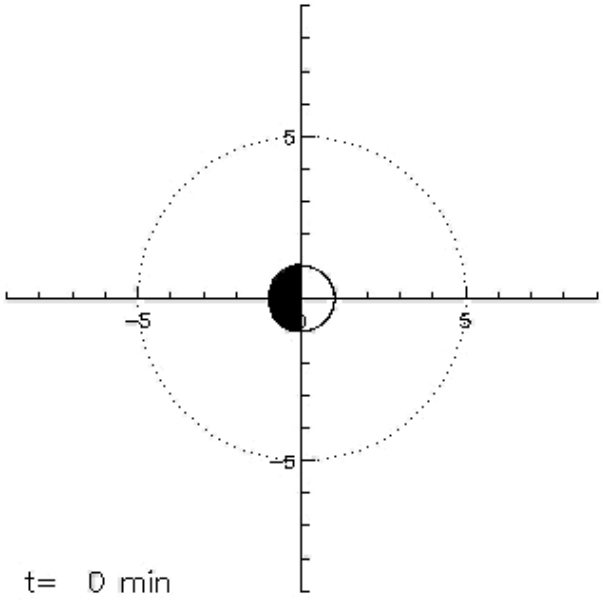

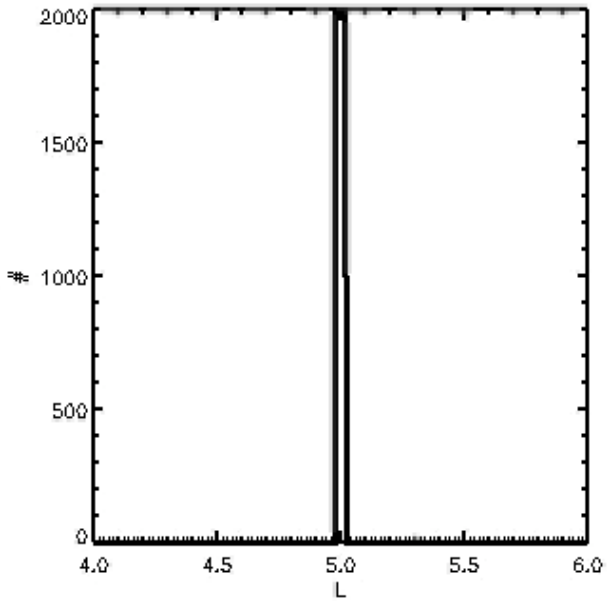

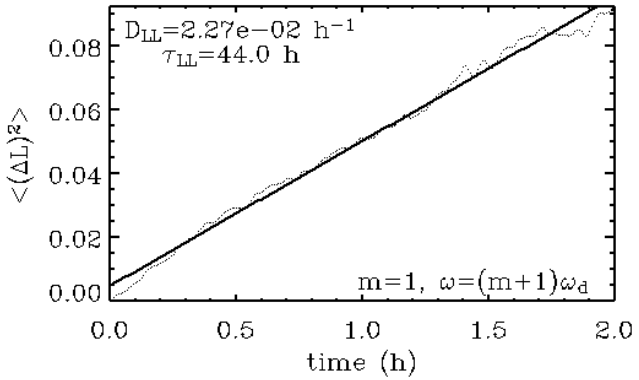

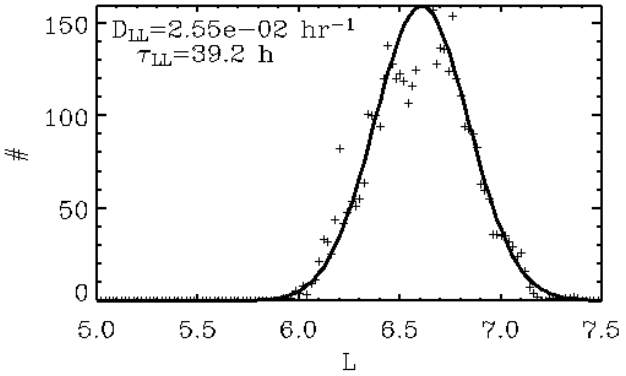

Ground-based Magnetometer ULF Wave Studies

Kara Perry and Mary Hudson

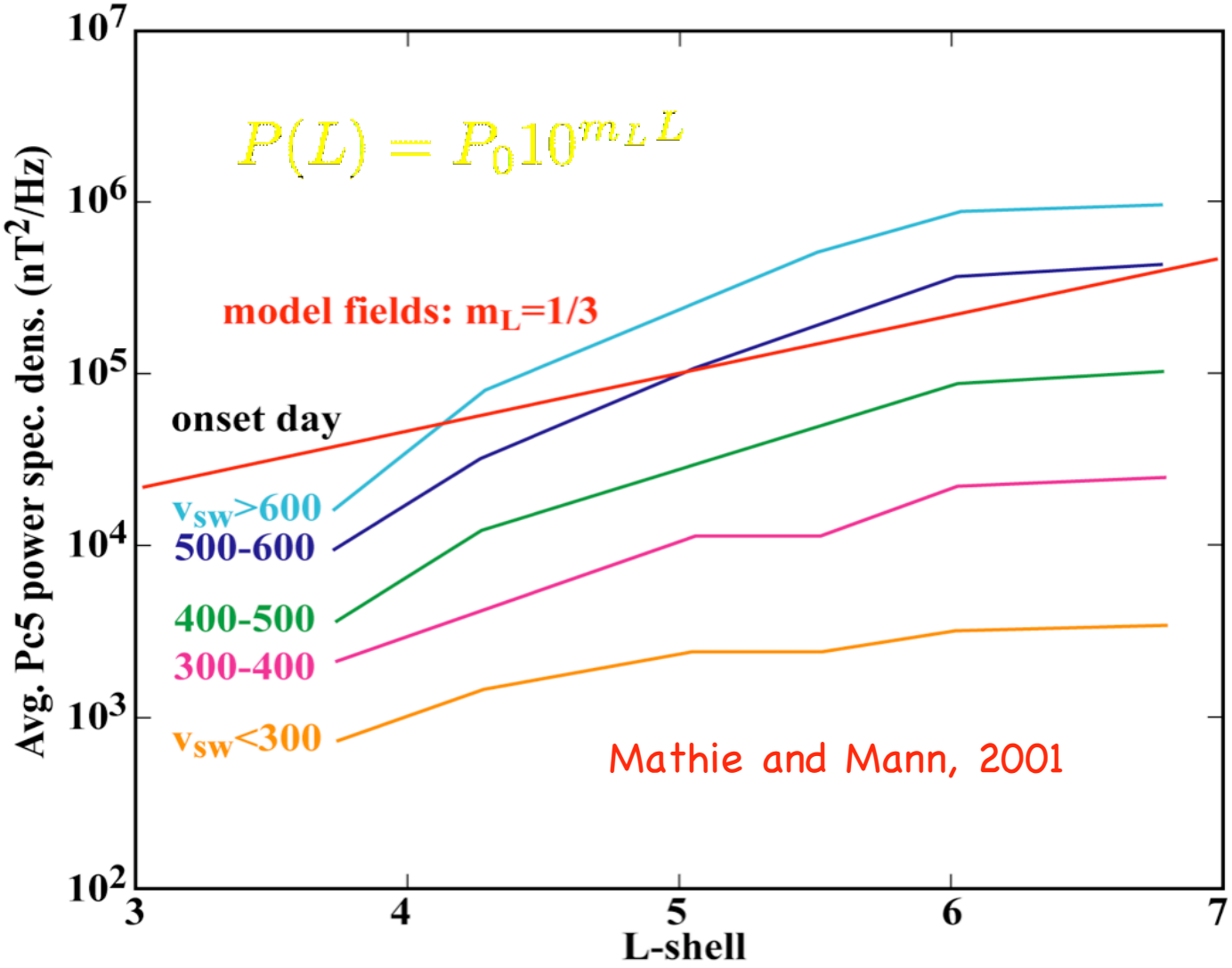

Evaluation of Diffusion Rates vs. L

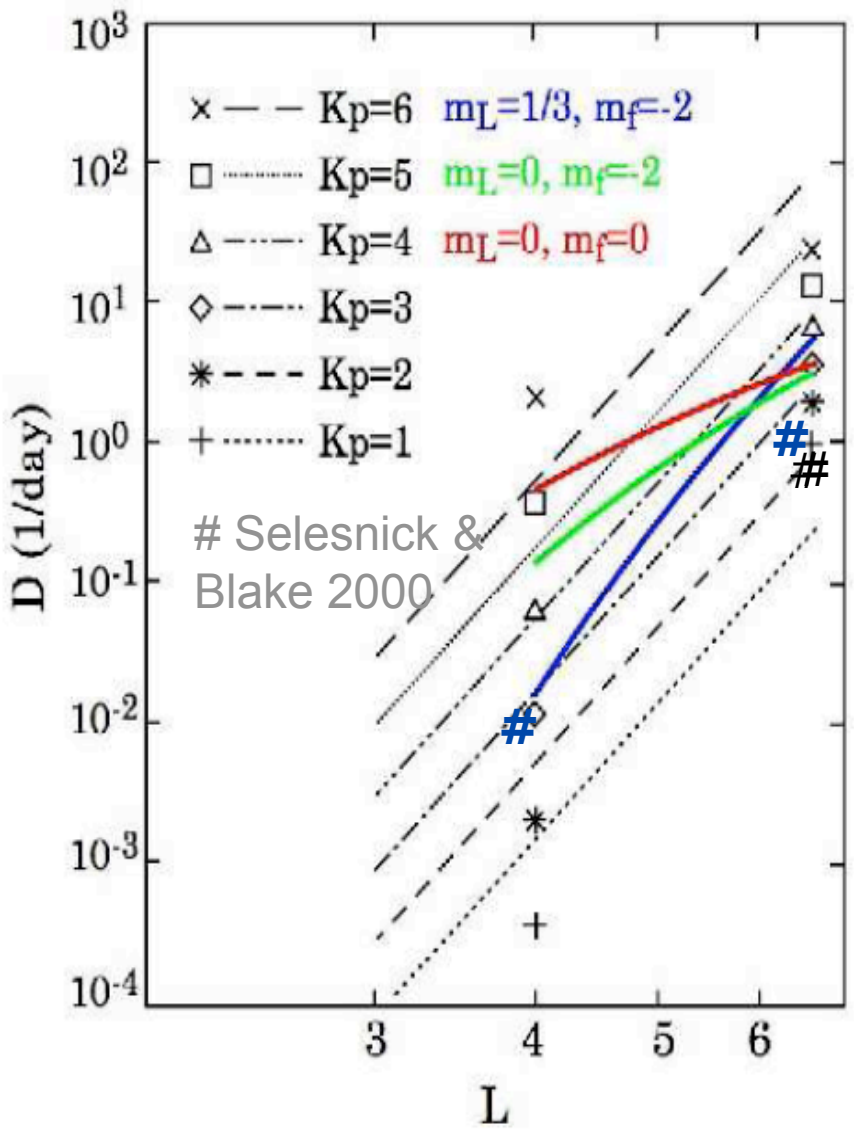

Perry et al., JGR, 2005,

Radial diffusion rates in model ULF wave fields
$D_{LL} \sim L^N$

Include E_ϕ, Br, B_{par},
freq and L-dependent power,
3D trajectories
N ~ 6 for no L-dep power, N ~ 12 with L dependence
M=273 MeV/G

Tau(L,E) is loss rate

$$\frac{\partial f}{\partial t} = L^2 \frac{\partial}{\partial L}\left[\frac{1}{L^2} D_{LL} \frac{\partial f}{\partial L}\right] - \frac{f}{\tau}$$

Braughtigam & Albert, 2000, N=6, 10; Perry et al., 2005, N=6, 12

Comparison of Radial Diffusion Times with Typical Loss Times

Shprits and Thorne, 2004

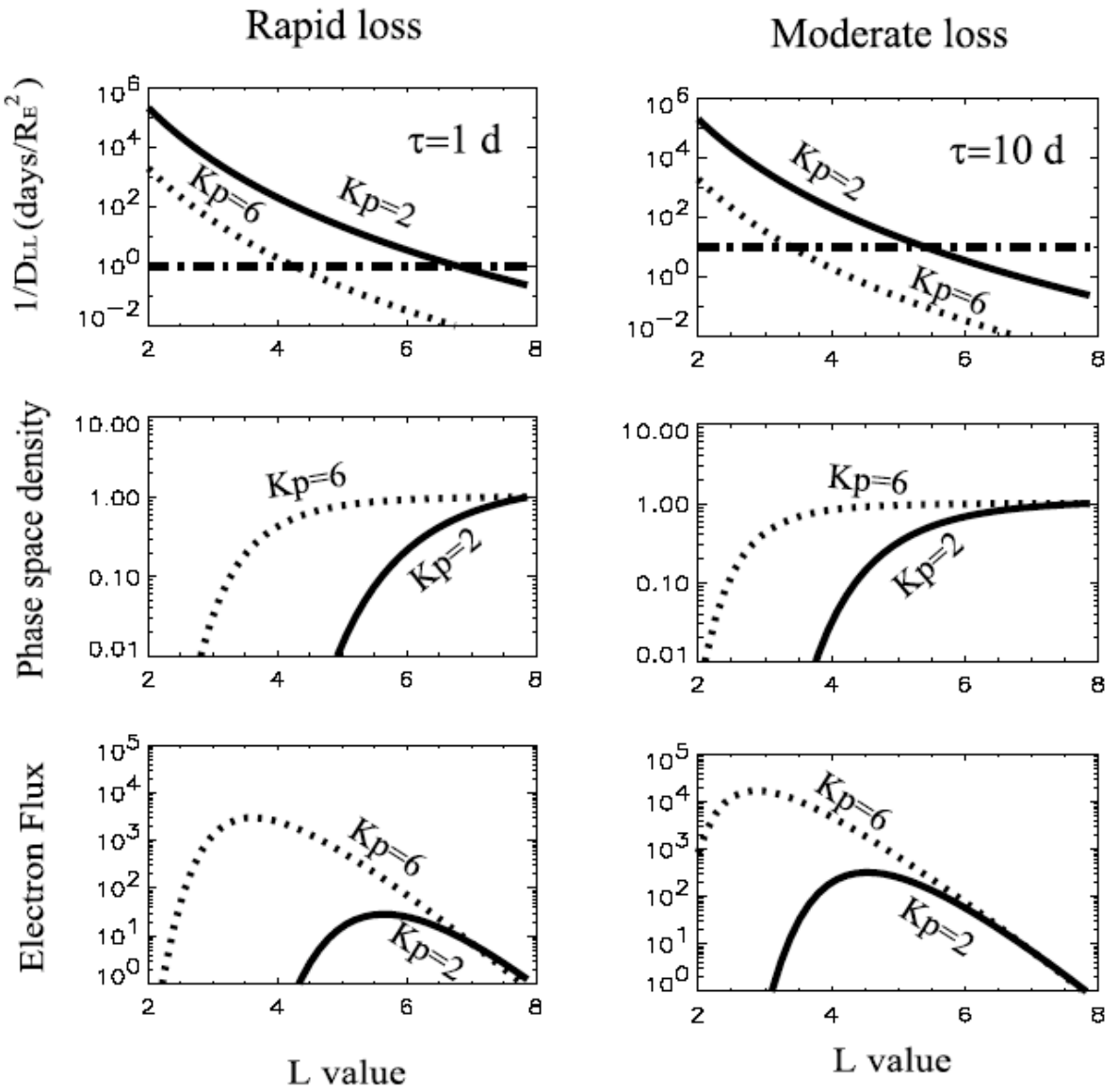

Radial diffusion dominates in the outer magnetosphere but losses dominate at lower L

Steady state solutions of the radial diffusion equation yield large gradients in phase space density when $D_{LL}\ \tau < 1$

Enhanced radial diffusion can lead to dramatic changes in electron flux at lower L

Radial Diffusion Simulation of CRRES Observations

Shprits et al., 2006

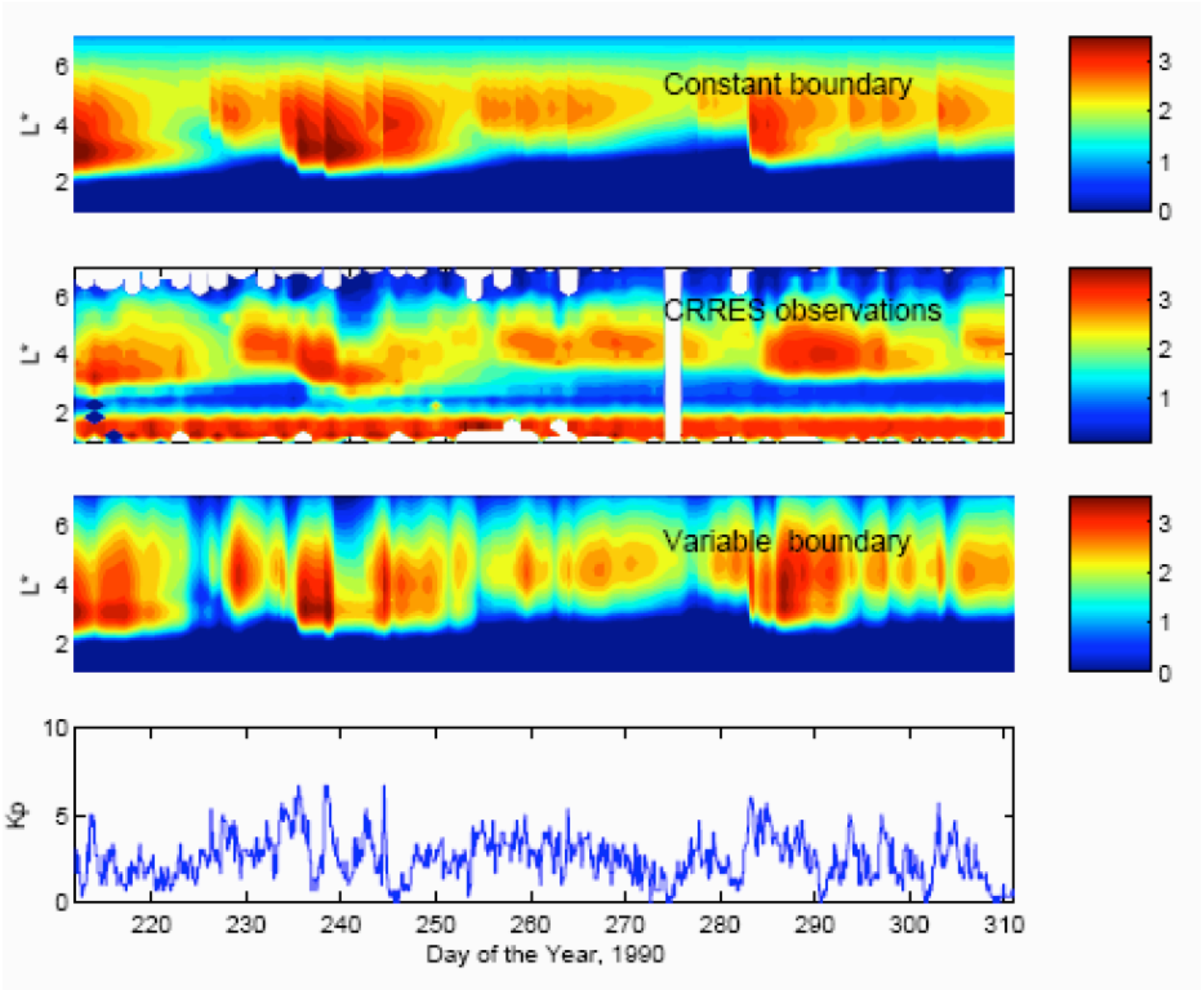

However Satellite Data shows Persistent Peaks in Phase Space Density: Evidence for Internal Acceleration

Green and Kivelson, 2004

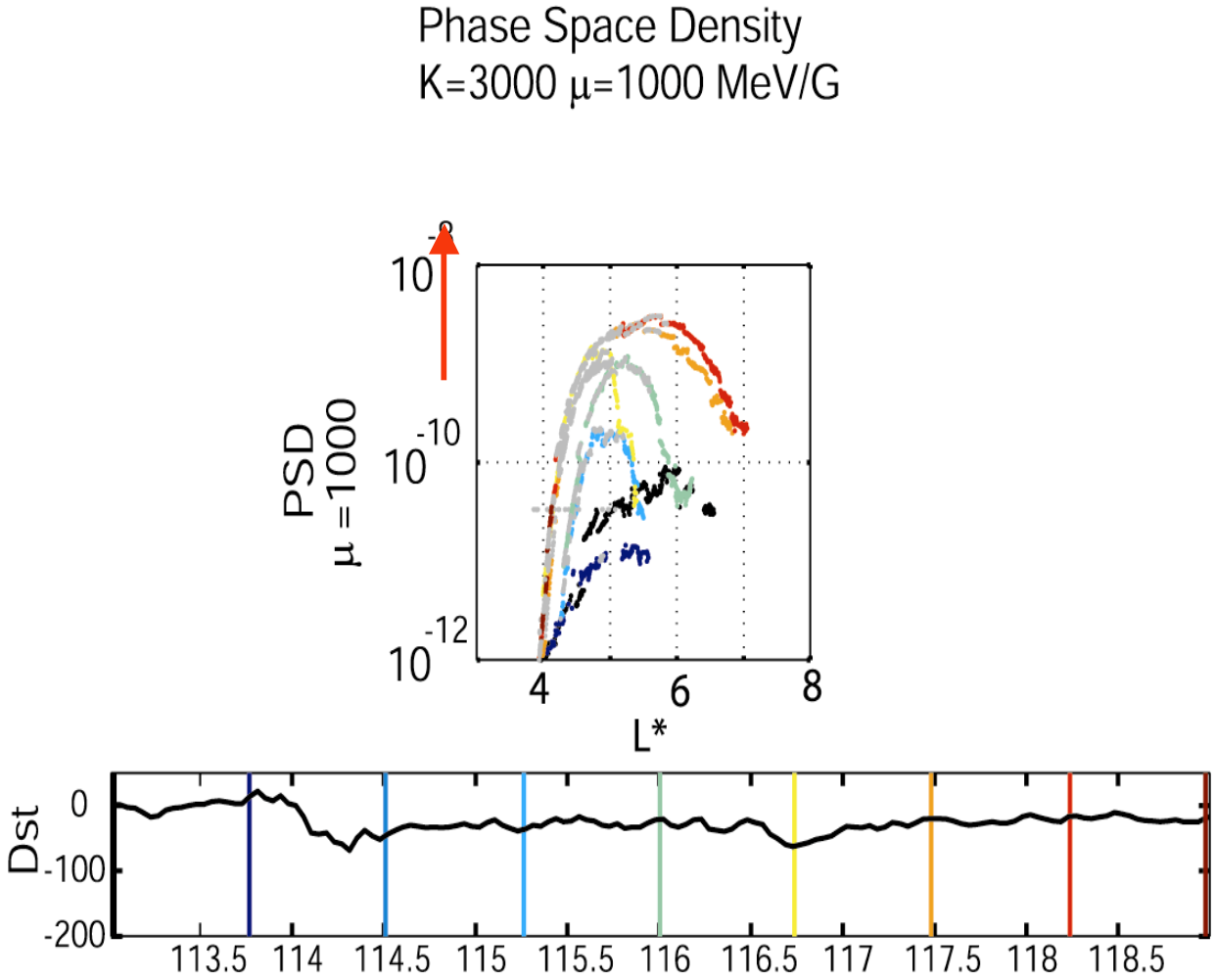

Enhancement in electron phase space density observed on Polar over a 3 day period in the recovery phase of a storm.

Evidence for Enhanced Whistler Mode Chorus Waves on CRRES During a Magnetic Storm

Meredith et al. JGR [2002]

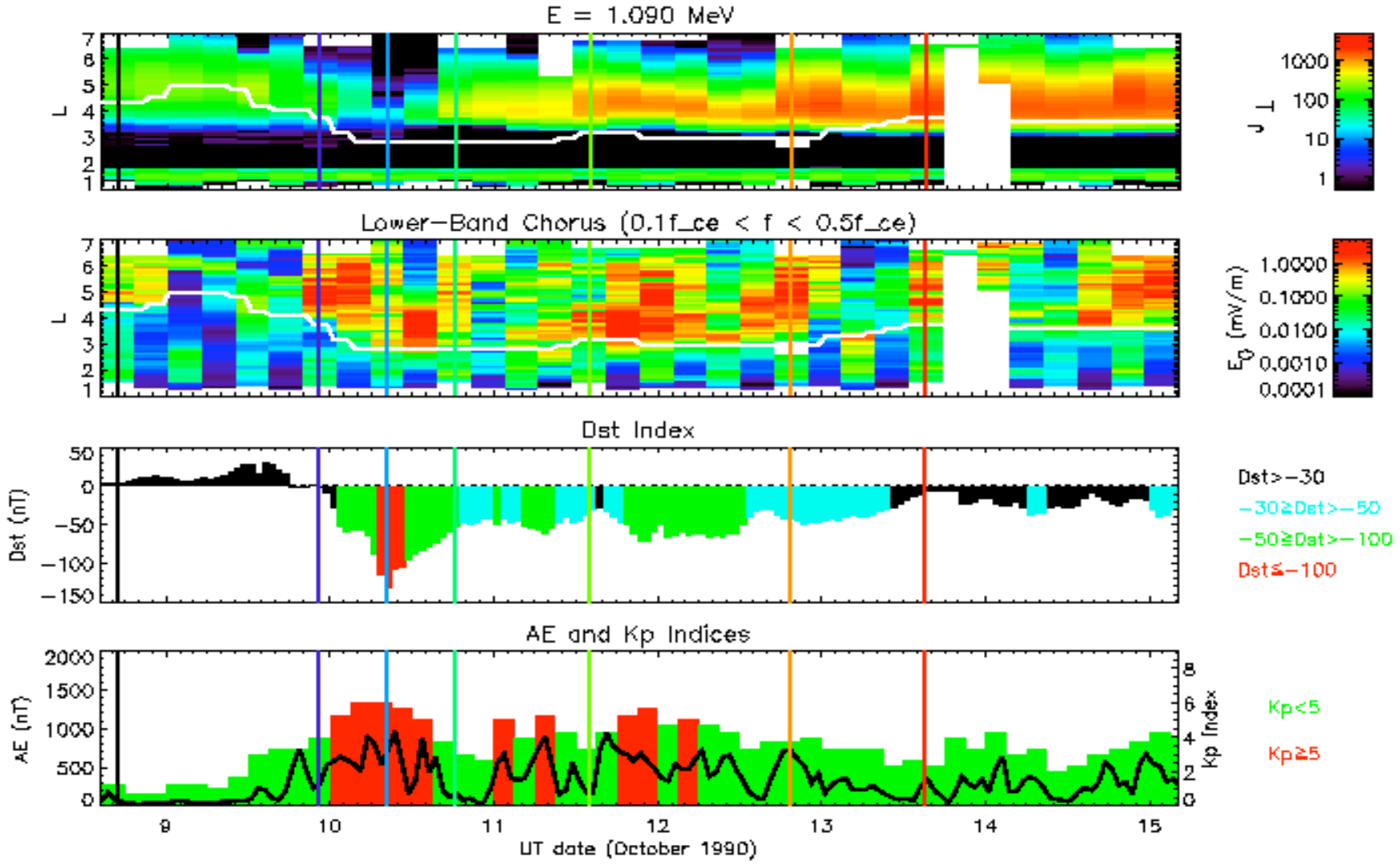

Concept of Local Stochastic Acceleration

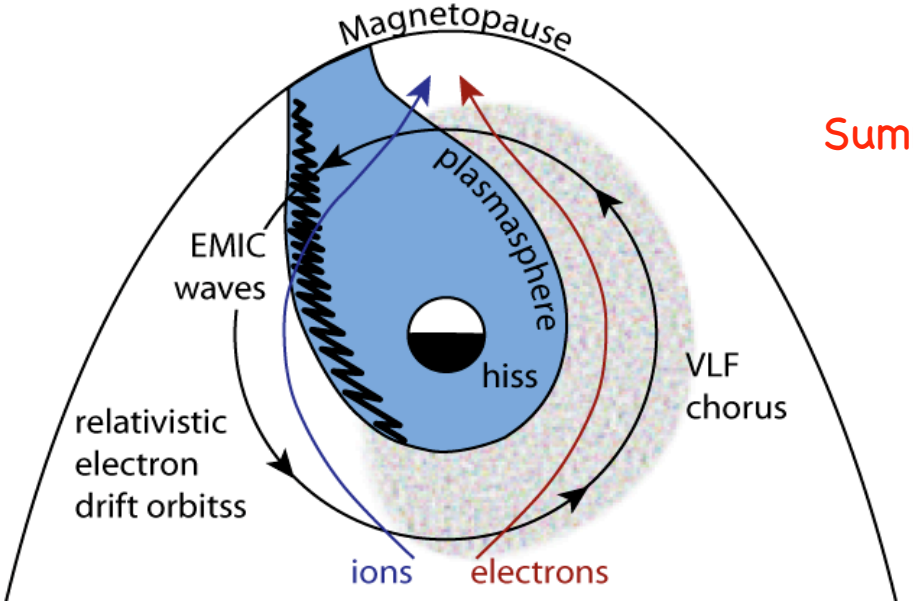

Summers et al., JGR [1998]

- Convection + radial diffusion inject ~1 - 100 keV electrons
  - Causes temperature anisotropy and excites whistler mode chorus
- Chorus accelerates a fraction of population to ~ MeV energies
  - Chorus + hiss +ion cyclotron waves contribute to loss to atmosphere

Acceleration by Whistler Mode Waves

- Electron diffusion into loss cone
  - Whistler wave growth
- At large pitch angles waves diffuse electrons to higher energy
  - Acceleration
- Minimum resonant energy for net acceleration when compared to loss

Horne and Thorne, GRL 2003

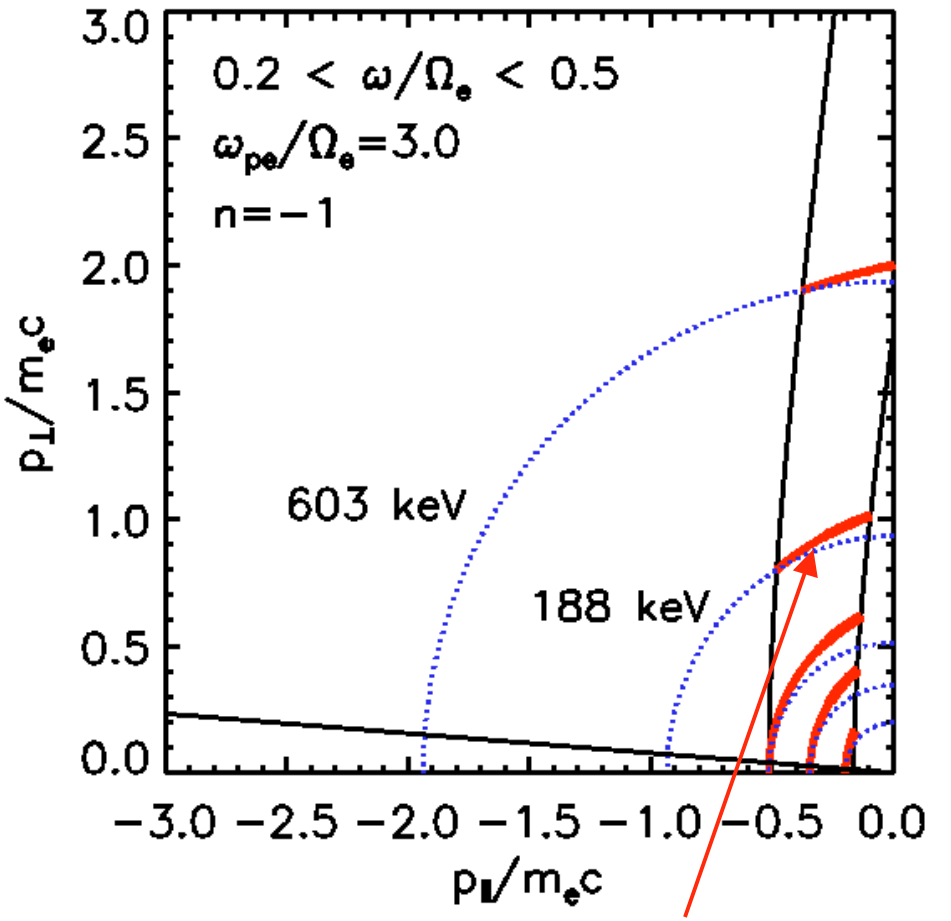

Resonant Diffusion Surfaces

Scattering Rates with the PADIE Diffusion Code

$$\frac{\partial f_0}{\partial t} = \nabla.(\mathbf{D}.\nabla f_0) =$$

$$\frac{1}{p\sin\alpha}\frac{\partial}{\partial\alpha}\sin\alpha\left(D_{\alpha\alpha}\frac{1}{p}\frac{\partial f_0}{\partial\alpha}+D_{\alpha p}\frac{\partial f_0}{\partial p}\right)+\frac{1}{p^2}\frac{\partial}{\partial p}p^2\left(D_{p\alpha}\frac{1}{p}\frac{\partial f_0}{\partial\alpha}+D_{pp}\frac{\partial f_0}{\partial p}\right)$$

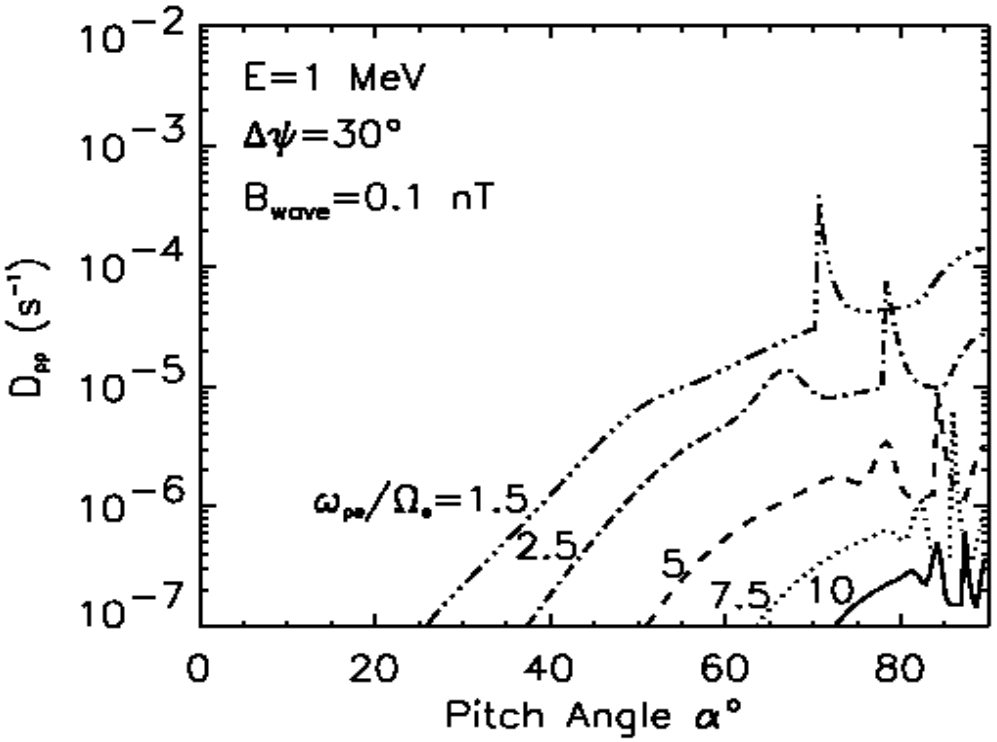

- Calculate pitch angle and energy diffusion rate.
- Momentum diffusion much more efficient for a low plasma density outside the plasmapause.

Horne et al. GRL, [2003]

Pitch-Angle and Energy Diffusion at 1 MeV

based on wave properties from CRRES, Horne et al., JGR 2005

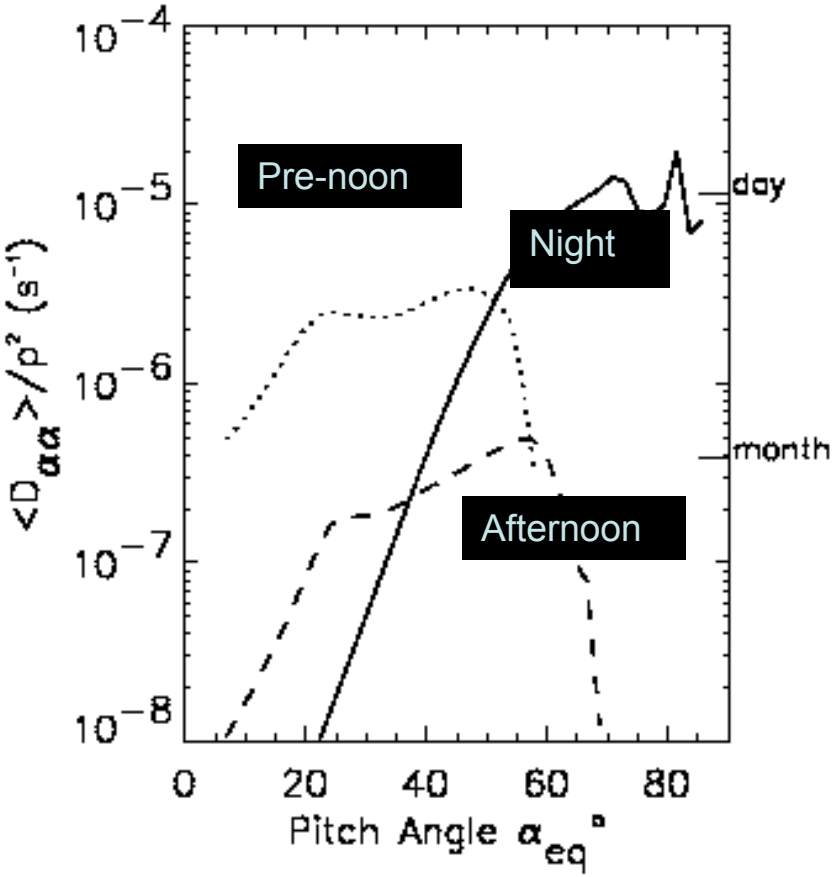

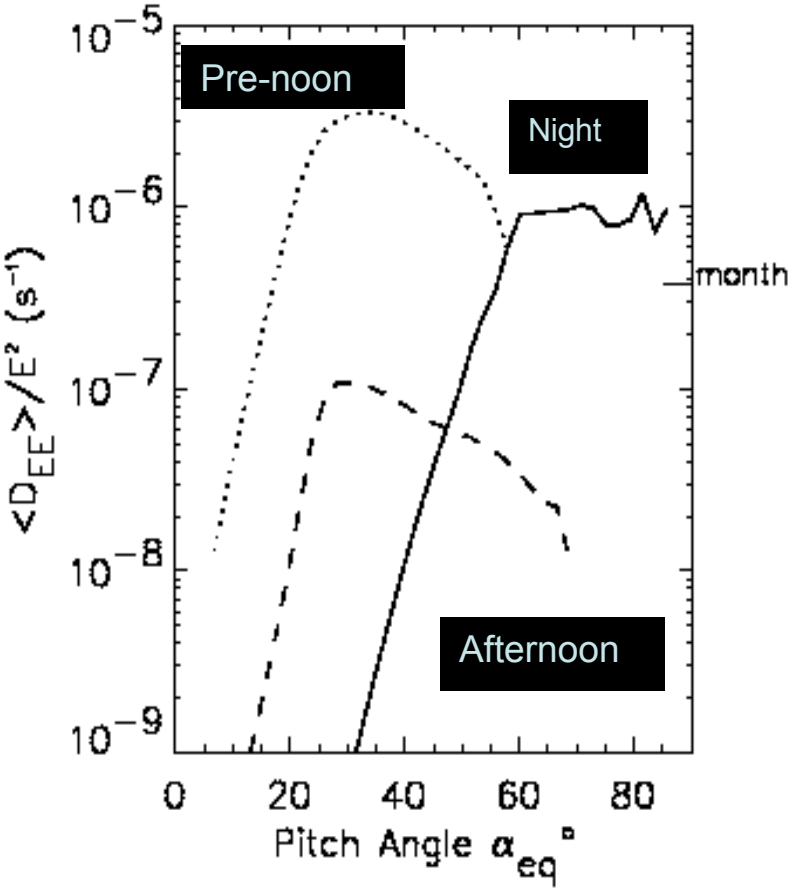

- Timescale for acceleration by chorus few days.
- Electrons accelerated faster than they are lost!

Self Consistent Wave Excitation with the RAM code

Vania Jordanova

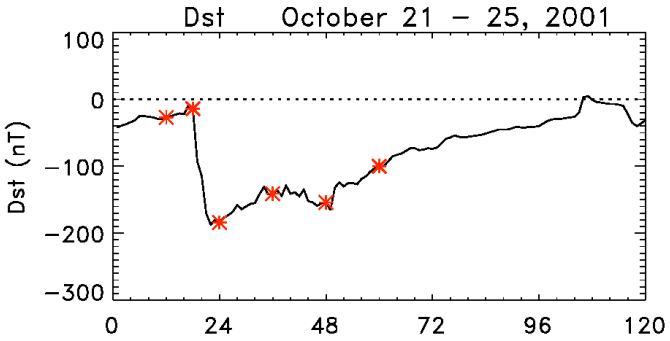

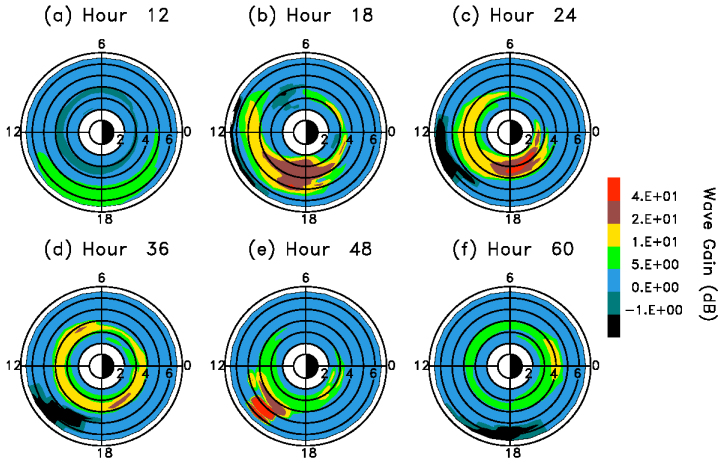

EMIC wave distribution
(from RAM-ion)

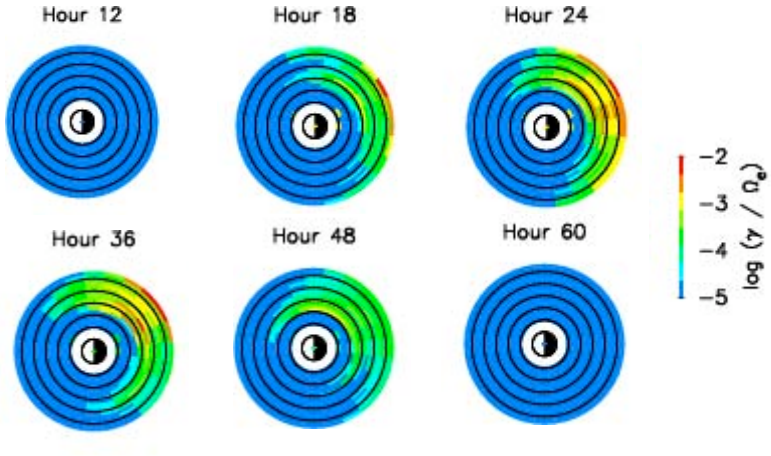

whistler mode wave distribution
(from RAM-e)

Developing a coupled ring current-radiation belt model including self-consistent wave-particle interaction with EMIC and whistler mode waves

Salammbo Code Simulation; Varotsou et al. GRL [2005]

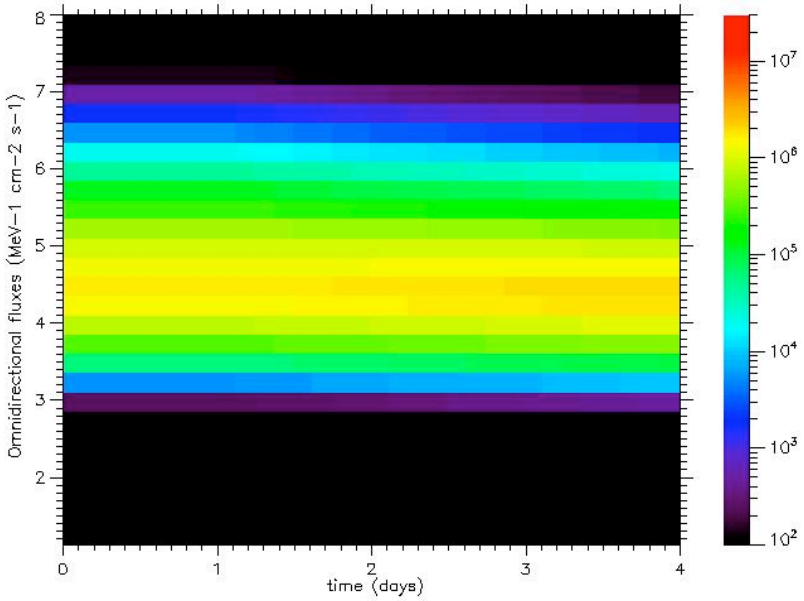

- Day 0-1 Kp=1.8 steady state
- Day 1-4 Kp=4 for 3 days
- 1 MeV flux
- Fixed outer boundary

1) Radial diffusion only

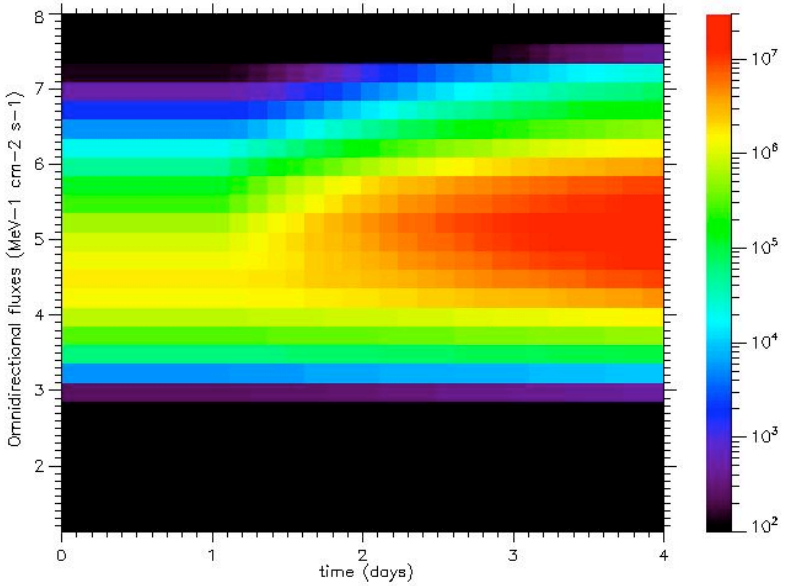

2) Radial diffusion and chorus scattering including loss and local acceleration

- Wave acceleration peaks near L=5
- Radial diffusion outwards, and inwards

Wave Acceleration in the Radiation Belts

Richard Horne

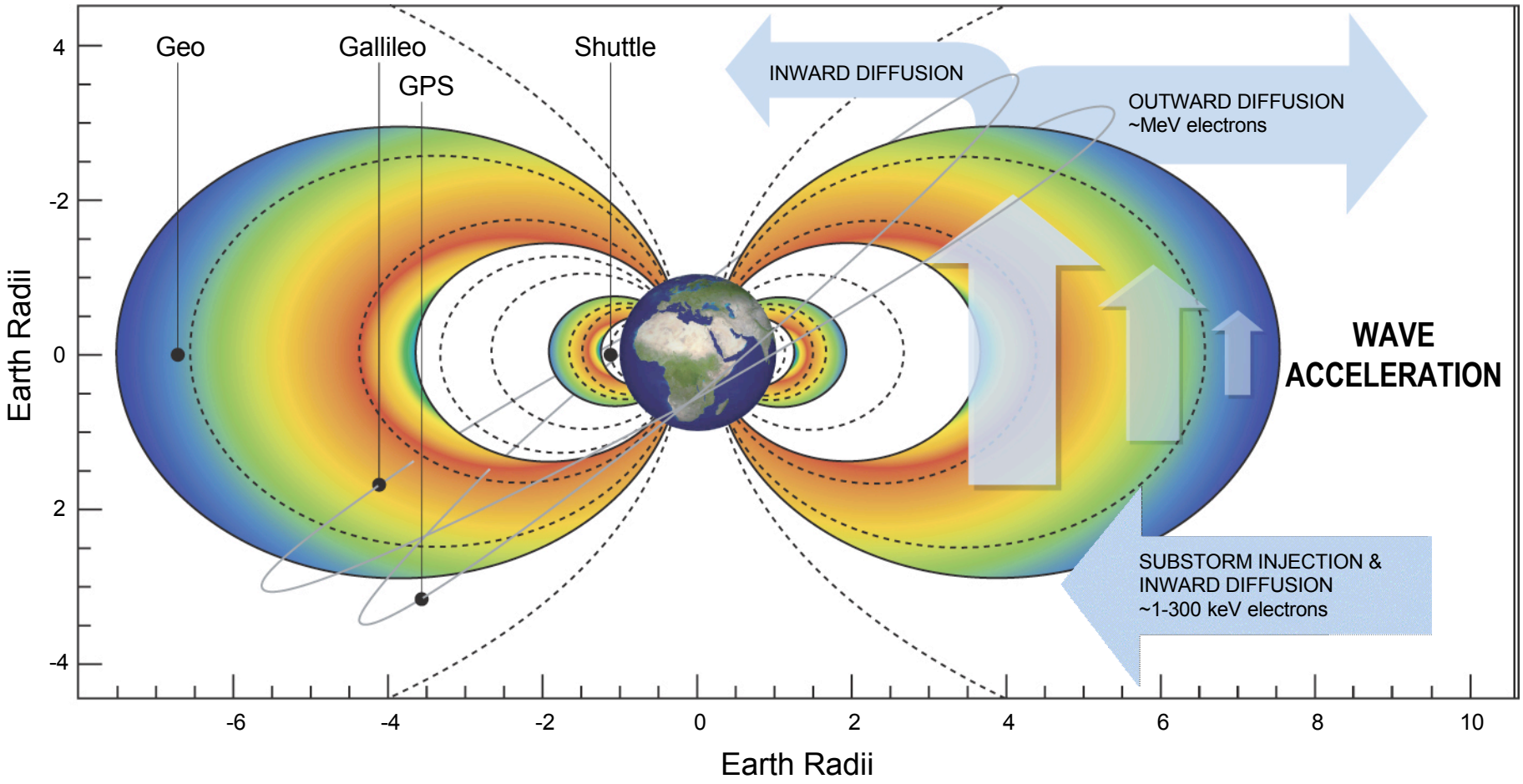

Effect on the Radiation Belts During the Halloween Storm

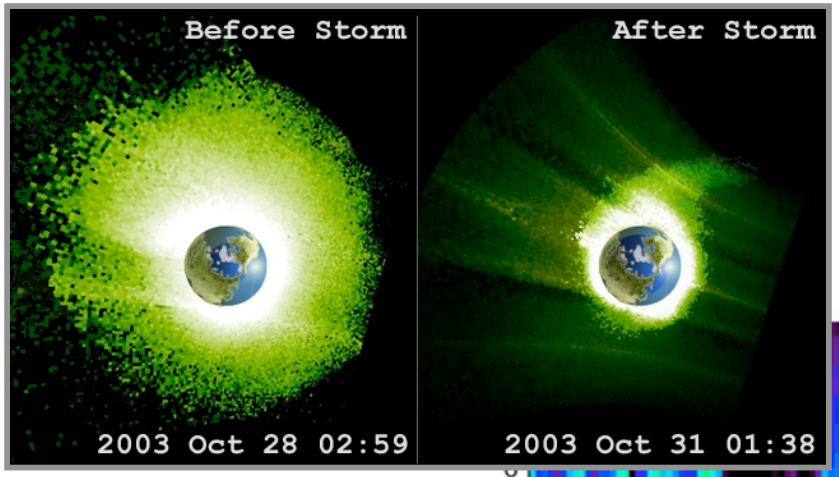

Baker et al., 2004, Nature

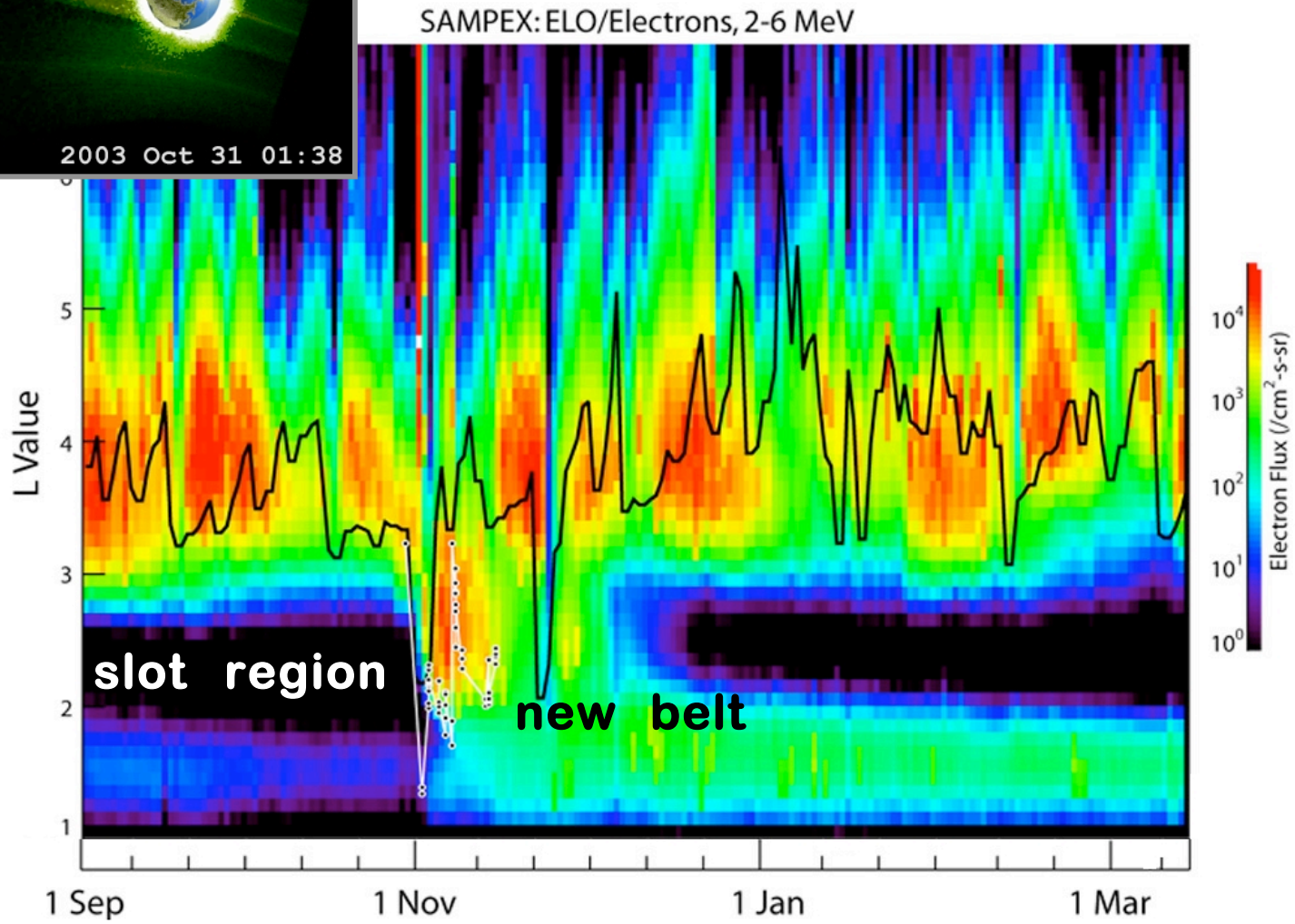

Radial Diffusion Rates During the Recovery Phase of the Halloween Storm

Horne et al., Nature 2005

Geomagnetic activity index Kp and Dst during the storm

ULF wave power

Radial Diffusion Rates peak during the main phase but decease dramatically during the recovery when relativistic electrons flux is strongly enhanced.

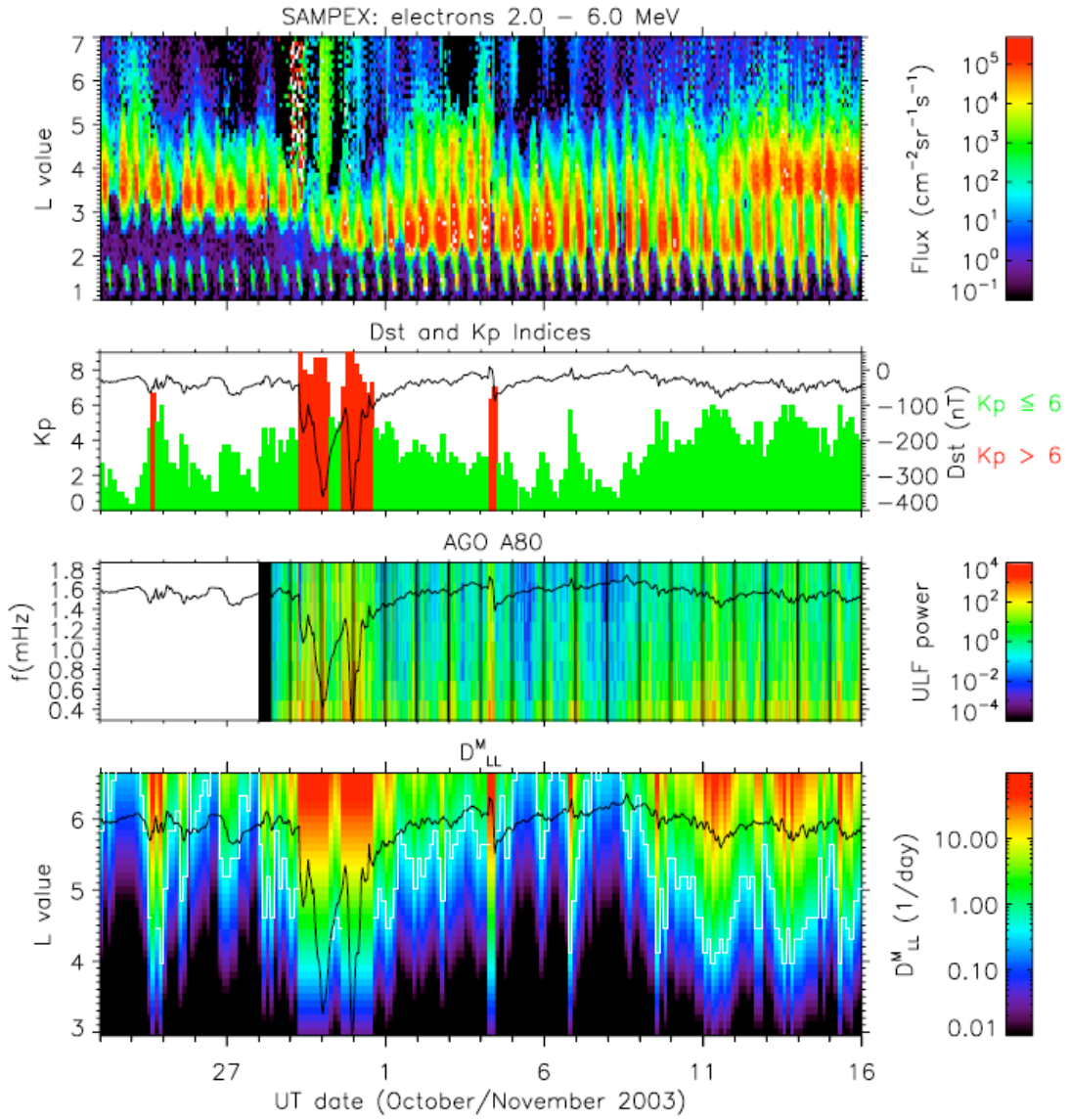

Evidence for Intense Chorus Emissions at low L during the Recovery Phase of the Halloween Storm

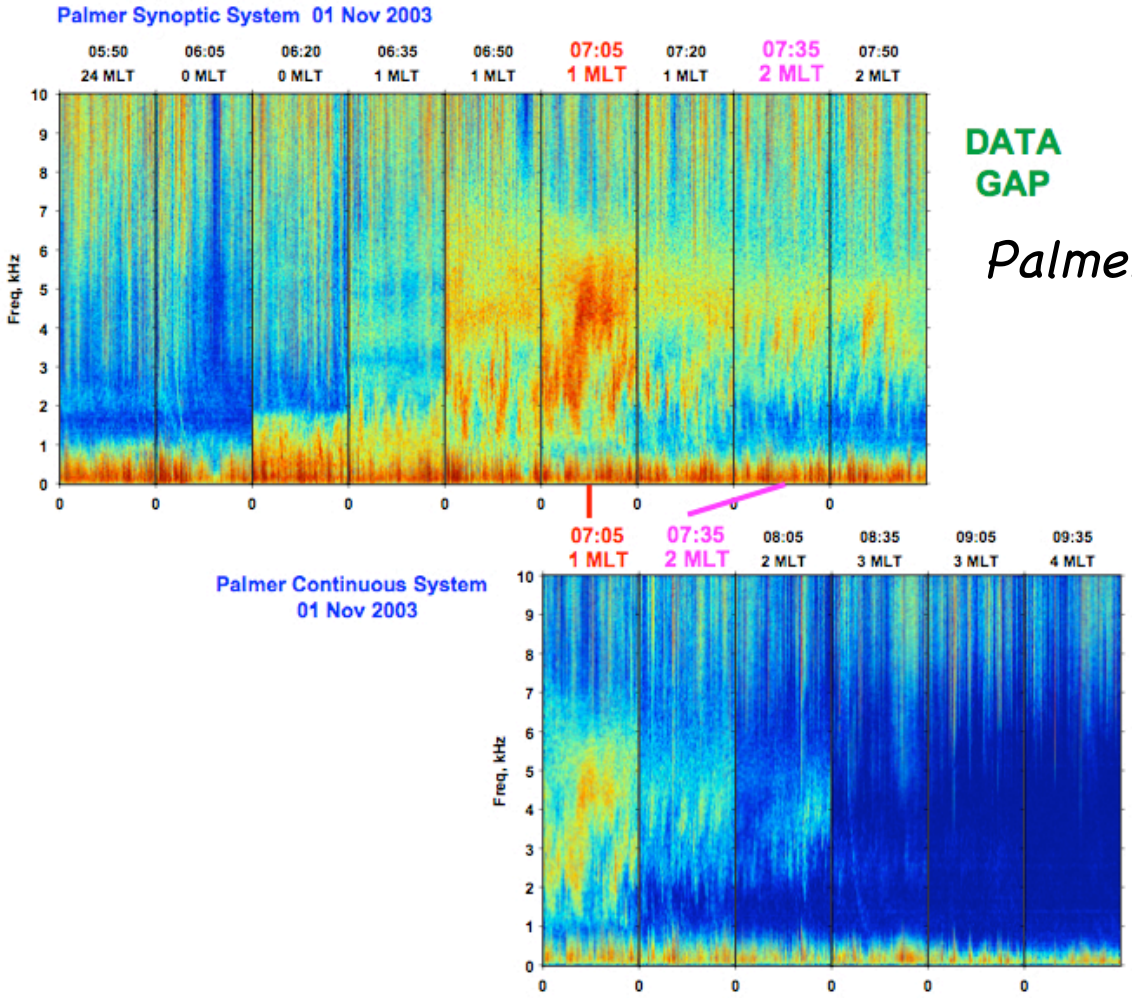

Energy Diffusion Rates and Local Acceleration Timescales Using the PADIE Code

B_w = 100 pT over 30 degs of latitude
at L=3 on the dawnside
N = 100/cc, Sheeley et al. 2001

$$\frac{\partial f}{\partial t} = \frac{1}{p^2}\frac{\partial}{\partial p}p^2 \tilde{D}_{pp}\frac{\partial f}{\partial p} - \frac{f}{\tau}$$

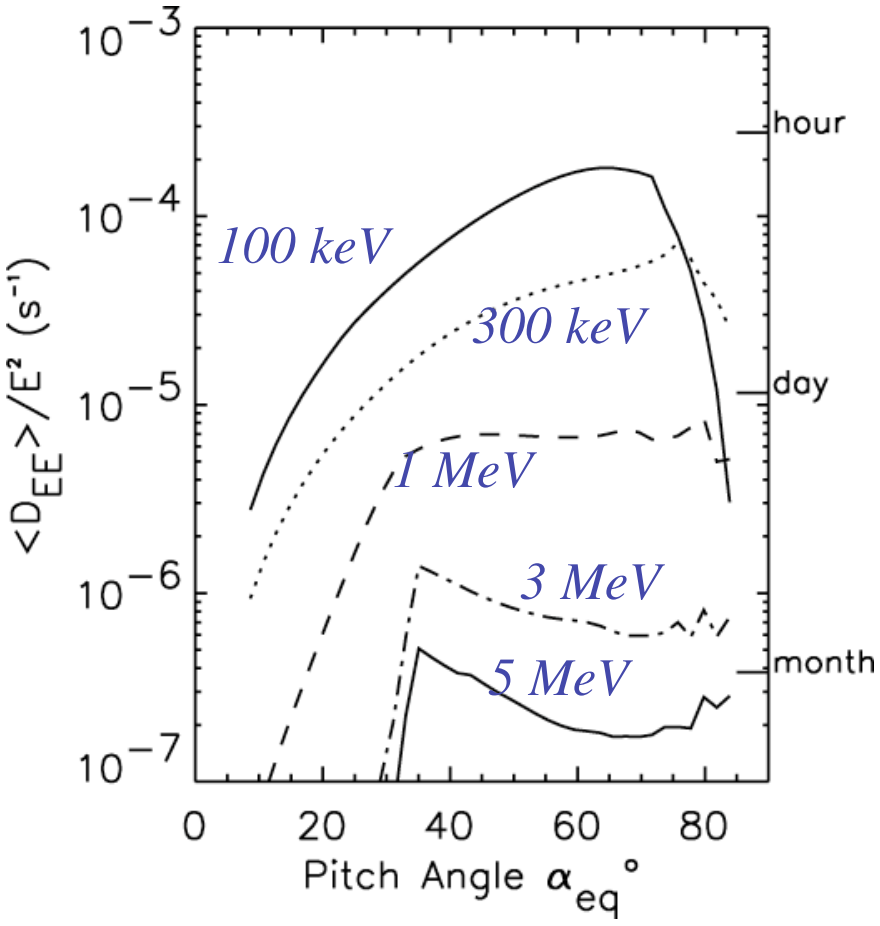

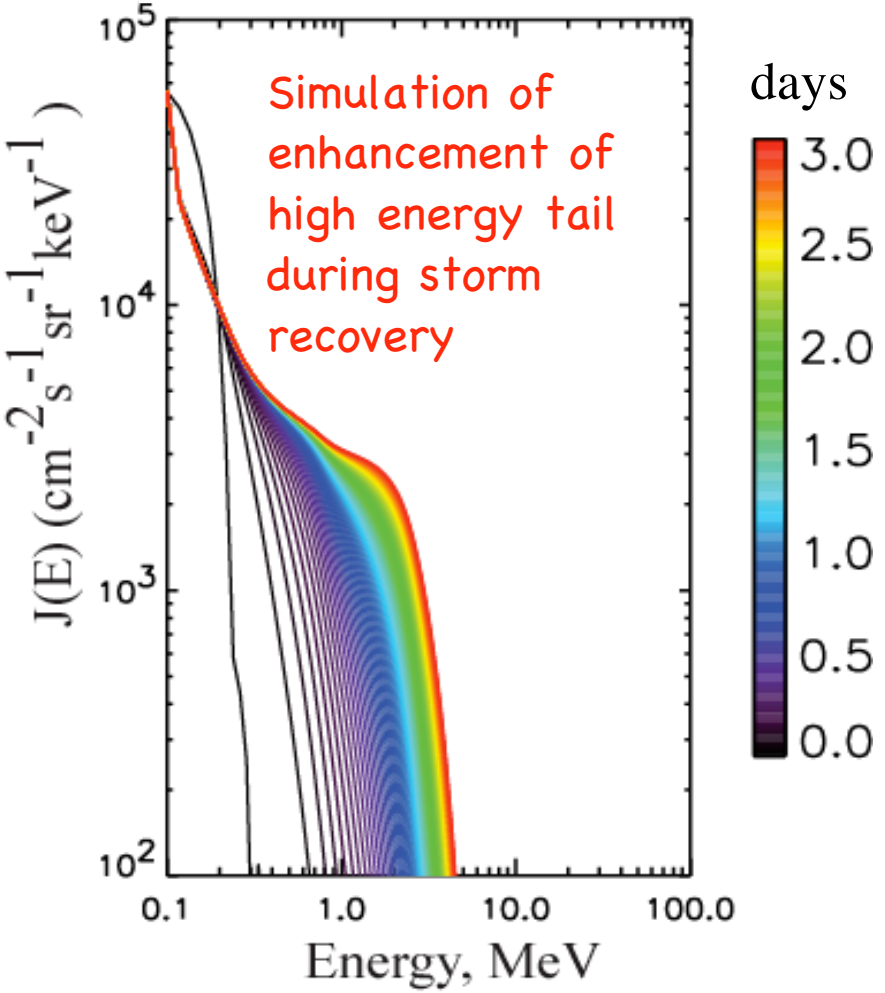

Conclusions

1) Several different waves are excited in the magnetosphere during geomagnetically active conditions and leading to non-adiabatic changes in the radiation belts.

2) EMIC waves, and whistler-mode chorus and hiss cause pitch-angle scattering and loss to the atmosphere. Net loss times for relativistic electrons can be less than a day during the main phase of a storm but much longer during the storm recovery.

3) Interactions with chorus emissions also leads to local acceleration and causes peaks in phase space density just outside the plasmapause.

4) ULF waves cause radial diffusion and associated particle energization during inward transport.

Unfinished Business: Where do we go from here?

1) We need to continue the development of 3D diffusion models, that incorporate all important physical processes and test them with satellite observations.

2) Diffusion codes require accurate global models for the polarization and power spectral characteristics of resonant ULF, ELF and VLF waves and their variability with geomagnetic activity. This will necessitate data mining and detailed analysis of available satellite observations.

3) Understanding the origin of plasma waves and their affect on the radiation belts with also require accurate models for the global distribution of plasma density and ion composition.

4) We must continue to support for the LWS RBSP mission, which will hopefully provide definitive new observations to address key questions on the source and loss process for the radiation belts.